BELLCOMM, INC.
1100 SEVENTEENTH STREET, N.W. WASHINGTON, D.C. 20036

COVER SHEET FOR TECHNICAL MEMORANDUM

TITLE- Unmanned MSSR Entry into Mars During the 1975 Manned Twilight Flyby

TM- 67-1013-7

DATE- September 20, 1967

FILING CASE NO(S)- 233

AUTHOR(S)- D. E. Cassidy

FILING SUBJECT(S)- Mars Missions
(ASSIGNED BY AUTHOR(S)- Entry Vehicles

ABSTRACT

The unmanned planetary probe employed in conjunction with a manned flyby mission substantially increases the information acquisition potential of both the manned flyby and the unmanned probe. In this paper, the design requirements and operational aspects of entry probes for application during a manned flyby of Mars are considered with particular emphasis on a Mars Surface Sample Return (MSSR). The effects of the entry environment, atmospheric uncertainty, and the terminal propulsive maneuver are investigated.

SEE REVERSE SIDE FOR DISTRIBUTION LIST

DISTRIBUTION

COMPLETE MEMORANDUM TO

CORRESPONDENCE FILES:

OFFICIAL FILE COPY
plus one white copy for each additional case referenced

TECHNICAL LIBRARY (4)

NASA Headquarters

Messrs. P. E. Culbertson/MLA
J. H. Disher/MLD
F. P. Dixon/MTY
W. B. Foster/SM
E. W. Hall/MTS
D. P. Hearth/SL
T. A. Keegan/MA-2 COPY
D. R. Lord/MTD
O. W. Nicks/SL
M. J. Raffensperger/MTE
L. Reiffel/MA-6
A. D. Schnyer/MTV
P. G. Thome/SL
G. S. Trimble/MT

MSC

Messrs. C. Covington/ET23
G. C. Miller/ET23
M. A. Silveira/ET25
W. E. Stoney, Jr./ET
J. M. West/AD

MSFC

Messrs. R. J. Harris/R-AS-VP
E. D. Messer/R-OM-V
B. G. Noblitt/R-AERO-DPT
F. L. Williams/R-AS-DIR

KSC

Messrs. J. P. Claybourne/EDV4
R. C. Hock/PPR2
N. P. Salvail/MC

Ames Research Center

Mr. L. Roberts/M (2 copies)

Jet Propulsion Laboratory

Mr. E. Pounder/126-140

Langley Research Center

Mr. C. J. Donlan/1219-106

Bellcomm, Inc.

Messrs. F. G. Allen
G. M. Anderson
A. P. Boysen
C. L. Davis
J. P. Downs
D. R. Hagner
P. L. Havenstein
J. J. Hibbert
W. C. Hittinger
B. T. Howard
D. B. James
H. S. London
K. E. Martersteck
R. K. McFarland
J. Z. Menard
I. D. Nehama
G. T. Orrok
I. M. Ross
R. L. Selden
R. V. Sperry
J. M. Tschirgi
R. L. Wagner
J. E. Waldo
All Members, Division 101
Department 1023

BA-146 (8-64)

SUBJECT: Unmanned MSSR Entry into Mars During the 1975 Manned Twilight Flyby - Case 233

DATE: September 20, 1967

FROM: D. E. Cassidy

TM: 67-1013-7

TECHNICAL MEMORANDUM

INTRODUCTION

The purpose of this memorandum is to underline the basic concepts involved in delivering an unmanned vehicle to the surface of Mars. Although the conclusions are general, attention will be directed toward a surface sample retriever payload (MSSR) which will have the additional criterion of a surface launch.

It is assumed that the MSSR will be operating in conjunction with a manned flyby mission. The base line mission utilized in this study is the 1975 Mars Twilight Flyby having an atmospheric entry velocity on the order of 32,000 fps. The 1976 to 1978 multi-planet flybys of interest (having both Mars and Venus encounters) have associated with them Mars entry velocities less than 25,000 fps. The 1975 Twilight Flyby, then, except for later twilight flybys, represents a worst case mission in terms of entry velocity and ascent vehicle impulse requirements, i.e., landed payload weight.

ATMOSPHERIC MODELS

The atmospheric models utilized in this study are the VM-7 and VM-8 models[1] developed by JPL from Mariner IV occultation data. The density-altitude profiles for the series are presented in Figure (1) along with the more recently published atmospheres from MSC.[2] It can be seen that the VM-7 and VM-8 model atmospheres represent an effective envelope to the MSC data. The lower scale height of the VM-8 atmosphere results in the highest structural loads and heating rates. The low surface density of the VM-7 atmosphere, almost half the surface density of the MSC 5mb and VM-8 atmospheres, results in the largest propulsive landing penalty.

The VM-7 and VM-8 atmospheres were used here to demonstrate feasibility with what presently appear to be the most severe conditions. It will be shown that under this worst set of conditions a successful landing can be mechanized. Although the Martian surface topography and roughness is poorly resolved, it is reasoned that large, relatively smooth areas such as exist on the earth and the moon will be identified either during earlier unmanned flights or several days prior to planetary encounter.

This latter approach seems quite feasible when a large aperture diffraction limited telescope is utilized on-board the manned mission module.

ENTRY REQUIREMENTS

In order to perform a successful landing on the Martian surface, a number of conditions must be met. The MSSR, or any atmospherically decelerated entry probe, must come close enough to the planet so that sufficient energy is dissipated in atmospheric (aerodynamic) drag for the probe to be captured. Due to the tenuous VM-8 atmosphere, however, (two orders of magnitude less dense than earth at 160,000 feet) the entry has to be made steep in order to reach low enough altitudes where sufficient drag force can be developed to reduce the probes velocity. On the other hand, coming in at too steep an entry angle does not allow enough time for aerodynamic deceleration, and results in terminal landing propulsion penalties. The ideal situation is to choose a corridor which guarantees capture by the planet and minimizes landing propulsion. There are additional constraints, of course, such as the structural load, heating load, and various operational aspects, e.g., range dispersion, which have to be considered. The range dispersion criterion, however, will be the only constraint in addition to terminal propulsion to effect the position of the corridor. The reason for this is that the heating and the structural loads, for unmanned systems, do not vary sufficiently within the corridor limits (defined later as 10 nautical miles) to have significant influence on the vehicle design.

In Figure (2), a 0 nautical mile corridor represents the overshoot limit, i.e., the shallowest ballistic trajectory (L/D = 0) which does not exit the atmosphere following initial entry. (The corridor is measured in nautical miles since it is a differential vacuum periapsis altitude.) The velocity at 20,000 feet altitude is indicative of the terminal propulsion requirements for a landing system and is used to illustrate the sensitivity of the terminal propulsion system to the entry corridor and ballistic parameter. In addition, the corresponding Mach numbers at 20,000 feet are indicative of the deployment conditions for a parachute retardation system. It is assumed here that Mach numbers above 1.5-to-2.0 require two stage systems, i.e., small supersonic decelerator and large subsonic descent chute, while above Mach 4 or so requires state-of-the-art improvements in decelerator systems.

For high ballistic parameters (M/C_DA), the probe velocity at an altitude of 20,000 feet in the VM-8 atmosphere increases quite rapidly as the corridor widens. At the low ballistic parameters, though, terminal conditions are achieved at 20,000 feet over a wide range of entry angles, making the velocity insensitive to corridor.

Although it would be desirable to enter near the shallow end of the corridor from a terminal propulsion consideration, large range dispersions and landing site uncertainties present operational constraints. This is apparent from Figure (3) where the range (measured along the planet surface from the initial entry point) is presented for a vehicle with a ballistic parameter of .8 slugs/ft^2. For an entry corridor capability of 10 nautical miles, entry angles between -18.1° and -18.9°, the landing site uncertainty due to corridor width is about $\pm$ 60 nautical miles for the VM-8 atmosphere. This uncertainty increases to $\pm$ 75 nautical miles when combined effects of both the VM-7 and VM-8 atmospheres are considered. The latter case includes the atmospheric uncertainty and assumes that no better atmospheric data will be obtained between now and the mission.

If the 10 nautical mile entry corridor is shifted to steeper angles, the increased terminal propulsion requirements are illustrated in Figure (4). Thus, to reduce the landing dispersion by 50% with a ballistic parameter of .8 slugs/ft^2 requires almost twice the landing ΔV based on the VM-8 atmosphere.

ENTRY CORRIDOR

A 10 nautical mile corridor, based on vacuum periapsis, appears reasonable for manned planetary systems guidance.[3] It is noted here that the corridor required for successful probe delivery is defined as the difference in periapsis altitude and not on the accuracy in estimating the state vector at the nominal entry time. The reason for this is that the entry angle is changing quite rapidly with altitude (or time), and that apparent entry angle errors result, even for an exact vacuum periapsis altitude, from inaccurate knowledge of the reference altitude (or time).

DECELERATION LOADS

The maximum decelerations during entry are presented in Figure (5) for a ballistic parameter of .8 slugs/ft^2 at various entry angles. In Figure (6) maximum decelerations are presented for the steep end of the 10 nautical mile corridor (γ = -18.9°) at various ballistic parameters. The increasing decelerations at the lower ballistic parameters are due to the more rapid slowdown at high altitude resulting in steeper effective entry angles, i.e., the low ballistic parameter trajectory deviates more from a straight line approximation. For entry within the 10 nautical mile corridor, then, decelerations can be kept within $40 g_{\oplus}$ for direct ballistic entry at 32,000 fps.

AERODYNAMIC HEATING

The heat transfer to the stagnation region in Figures (7) and (8) is due to radiation as well as convective transport. The radiation load was assumed to originate in an optically thin adiabatic shock layer, and the magnitudes were computed from a correlation of CO_2-N_2 gas mixtures.[4] Although the radiation load in the stagnation region is considerably lower than the convective load for a 1 foot spherical nose, consideration must also be given to the heating distribution over the heatshield. In CO_2-N_2 gas mixtures, the CN molecule contributes substantial radiation emissions at temperatures associated with a velocity range from 25,000 to 34,000 fps resulting in higher radiant energy levels for CO_2-N_2 mixtures than for air mixtures. Radiation emissions from air fall off quite rapidly with velocity in this range. The effects of this phenomena are that in CO_2-N_2 mixtures gas radiation is less sensitive to velocity variations between 25,000 and 34,000 fps, and therefore maintains near-stagnation point levels around the entry vehicle body. When this effect is coupled with the increasing shock wave stand-off distance around the body (expanding plasma volume), higher radiation heating rates are experienced toward the maximum diameter than at the stagnation point.[5]

Approximations were made to the total convective and radiative distributed load. The radiative distribution was derived from a consideration of Reference 5, and the convective distribution followed Lees.[6] As a result, it was determined that the radiation load (considering non-adiabatic effects) will be about half of the convective load for the MSSR with a 20' diameter.

VEHICLE CONFIGURATION CONSIDERATIONS

The entry vehicle aeroshell chosen for this study is a blunted cone with a 60° half angle and a spherical nose.[7,8] The advantage of this shape is in its high drag coefficient and, therefore, low characteristic ballistic parameter. The packaging characteristics of spherically blunted cones are discussed in Reference 8.

In Figure (9), a 60° blunted cone is analyzed for payload capability at different ballistic parameters. The bottom curve is for a system which utilizes a terminal propulsion system, but no parachute retardation. The upper band includes the effects of using a large single ribbon chute ($M<1.5$) or a two stage supersonic plus ribbon chute. The single stage chute represents about 10% of the descent weight while the two stage system is approximately 20%. Both systems utilize terminal propulsion for landing.

Although the addition of a parachute system offers potentially higher payload fractions than the pure propulsion system, the increased complexity in light of the necessity for having a terminal propulsion system for a soft touchdown makes their use questionable. It was decided, then, to pursue this analysis with a pure propulsion system, leaving the advantages or disadvantages of parachutes in abeyance.

PAYLOAD CAPABILITY

The ballistic parameter which yields the maximum payload fraction for a pure propulsion system is about .55, Figure (9). For a 4000 pound MSSR ascent weight (4000 pounds is approximately the lift-off weight required to deliver a 42 pound payload to the manned flyby mission module, Reference 9), a ballistic parameter of .55 requires a 22.5 foot diameter entry vehicle, and a gross entry weight of just over 10,000 pounds. Increasing the ballistic parameter to .8, for the 4000 pound payload, results in a 3 foot reduction in the maximum diameter, although a 1000 pound increase in entry weight is required. The propulsion system fraction increased from about 16% to 26% of the entry weight; the structural plus heatshield fraction reduced from 36% to 31%. The structural and propulsion system fraction are presented in Figure (11).

It was assumed in the weights analysis that about 20% of the payload weight, i.e., ascent weight, is required for landing gear, payload support structure, no-return science and contingencies. No hover capability was programmed since a direct landing similar to the Surveyor system was assumed. If a T.V. link could be established between the manned flyby module and the landing MSSR, additional propellant for a site selection hover period would be desirable for providing local terrain clearance capability.

A ballistic parameter of .8 slugs/ft^2 appear to provide a reasonable compromise in payload fraction and packaging efficiency and will therefore be pursued in greater detail.

REFERENCE TRAJECTORIES

The reference trajectories for the .8 slugs/ft^2 ballistic entry at -18.9° (steep side of the 10 nautical mile corridor) are presented in Figures (12), (13), and (14). Below 50,000 feet altitude the plots are expanded in Figures (15), (16), and (17), to show the effects of atmospheric uncertainties and entry corridor (γ = -18.1° to -18.9°) on the thrust initiation conditions. The shading is employed to highlight the effects of the 10 nautical mile corridor width. For a time reference below 50,000 feet altitude, altitude versus time from entry is presented in Figure (18). Above 50,000 feet, time hacks are provided in Figure (12). In addition, the time histories for the stagnation point radiative (adiabatic) and convective heating rates are presented in Figure (19). The corresponding integrated heating loads can be determined from Figures (7) and (8).

NOMINAL POWERED DESCENT

For purposes of analysis, the following mode of retro fire and descent will be investigated.

1. Ballistic entry down to initiation altitude.

2. Initiate maximum (constant) thrust down to a constant deceleration reference trajectory. A constant deceleration reference is used as a simplified "patching" contour to allow the descent system to adapt to the variable end conditions resulting from entry corridor and atmospheric uncertainties.

3. Modulate thrust to maintain a constant deceleration to produce a nominal soft touchdown.

The heat shield will be separated before touchdown, sometime after its weight exceeds its drag force. It is desirable to have a low dynamic pressure on the heatshield at separation to minimize separation forces and reduce any tendency of the heat shield to be destabilized by the flow field. In addition, a forward facing rocket firing upstream of the heat shield will disturb the flow field and change the drag and stability characteristics of the vehicle. The effects of potential drag reduction on landing performance will be considered here, although it appears that a proper choice of configuration could actually produce a drag amplification. It is assumed that any destabilizing moments can be handled with rocket augmentation.

To date, there has been little experimental work done on the subject of forward facing jets. Presently, however, it appears that a rocket plume aligned along the center line of a blunted entry cone will reduce the drag of the cone, Reference (10), but rockets located circumferentially around the periphery of the cone will increase the drag, Reference (11). Experimental results on a 60° cone for peripherally arranged rockets and a blunted configuration with a near centerline arrangement are presented in Figure (20) for various ratios of exhaust total pressure to free stream total pressure. The wide differences between the two sets of data, i.e., vehicle configuration, pressure ratios, and Mach numbers, make direct comparison very difficult.

THRUST-TO-WEIGHT REQUIREMENTS

The thrust to entry weight ratios required to achieve a zero velocity at 400 feet altitude with a constant thrust level (no drag attenuation) is presented in Figure (21) (solid lines), for various ignition altitudes. (An altitude of 400 feet was chosen as a nominal reference cut-off altitude.) The initial entry trajectories were computed along the steep side of the 10 nautical mile corridor and consider the effects of both the VM-7 and VM-8 atmospheres. Following thrust ignition, the thrust vector

was aligned with the velocity vector throughout the descent, resulting in a gravity turn. Although this is not an optimum (lowest propellant) descent, it represents a reasonable estimate of the operational and propulsion system requirements.

The corresponding propulsion system fractions are presented in Figure (22). The propulsion system fraction is based on a storable propellant specific impulse of 315 seconds and a propellant loading of .85.

The effects of reducing the drag to 60° of nominal (across the Mach number range) and reducing the drag to zero following retro ignition are also included in Figures (21), and (22) for the VM-7 atmosphere. For the zero drag case, the increased thrust-to-weight requirements at the high ignition altitudes are due to the absence of substantial drag losses. This condition results in higher average velocities (and therefore shorter times) from thrust ignition to termination. If indeed, the drag is substantially reduced, than higher thrust-to-weight ratios would be required for center firing rockets than for peripheral rockets.

The nominal thrust-to-weight chosen for the remainder of the work is 1.5 based on the VM-7 atmosphere, full drag case. These conditions result in a propulsion system fraction of .26 of entry weight and an ignition altitude of 17,000 feet. The solid curves on Figure (23) are the resulting powered descent trajectories where thrust was initiated at 17,000 feet. The dashed curves are constant deceleration reference trajectories, based on vertical descent, which result in a soft touchdown. Transition from the high thrust leg to the low thrust leg (reference contour) could be commanded using a recursive feedback control network, for example. Surveyor type RADVS (altitude and doppler) signals would be compared with the reference contour and a statistically weighted least squares error signal would command the required thrust history.

For the design case, $\gamma = -18.9°$, VM-7 atmosphere, the solid circle on Figure (23) indicates the point where the engine (or engines) could be reduced from a T/W = 1.5 to approximately .5 for a soft touchdown. The open circles are possible transition conditions accounting for the corridor width and assuming that no better atmospheric data will become available, i.e., the VM-7 and VM-8 are equally likely representations of the Martian atmosphere. If, indeed, the VM-8 model better describes the Mars atmosphere, the vehicle could encounter the reference contour at a velocity as high as 250 fps at an altitude of 8,000 feet. Maintaining a T/W = .5, then, would utilize propellant at a low thrust level which is available from the main propellant tanks and would introduce no propellant penalty. The reason for this is that the lower velocity in the VM-8 atmosphere more than offsets the increased gravity loss during the low thrust descent. On the other hand, if the main retro was a solid and the low thrust

rockets liquid, unused main retro propellant could not be used for the low thrust rockets. In this case, additional propellant for about 700 fps would be required to follow the reference contour.

THRUST INITIATION

The scheme suggested here requires a knowledge of the vehicle's altitude in order to determine the point of ignition. Other ignition signals could also be employed, e.g., velocity or slant range. It is felt, however, that the altitude initiation scheme contains the basic elements required to demonstrate feasibility and point out some of the operational considerations.

Since the vehicle is descending at high velocity through the Martian atmosphere, it is enveloped in an ionized plasma. It is expected, therefore, that a communications blackout will occur for some period during the initial entry when radar ground tracking is not possible. The critical velocity where electromagnetic waves will begin to propagate beyond the flow field (exit from blackout) at sufficient power levels to track the ground is a complex function of atmospheric composition, vehicle shape and transmission frequency. A conservative estimate to the critical velocity was made at about 10,000 fps. It will be shown that increasing this value to 15,000 fps will increase the ground acquisition and tracking time by about 15-to-20%.

For a critical velocity of 10,000 fps, the vehicle will start transmitting and receiving tracking data (altitude and Doppler rates) anywhere from 38,000-to-52,000 feet altitude for the VM-8 atmosphere and 63,000-to-75,000 feet altitude for the VM-7 atmosphere, Figure (12). For a nominal thrust initiation altitude of 17,000 feet, then, there is a minimum tracking time between the start of ground track and retro ignition. This time is 30 seconds for the VM-8 atmosphere and 60 seconds for the VM-7. These times increase to 37 seconds and 70 seconds, respectively, if the critical velocity is increased to 15,000 fps. Although the VM-7 atmosphere, as previously discussed, determines the retro and propellant requirements, the VM-8 atmosphere will determine the minimum tracking time.

It is anticipated that a pulse-type radar similar to the Surveyor system will have sufficient time, within the minimum 30 seconds, to mark the proper ignition altitude utilizing a simplified signal integration system. The pulse-type radar, though, will have to be roll-attitude stabilized in order to insure that the radar is pointing down, or redundant systems will have to be employed peripherally around the vehicle to determine the minimum range, i.e., altitude. A forward facing pulse radar would probably be undesirable due to the shallow flight path angles (-10°-to--19°) at 17,000 feet, Figure (17), and possible perturbations to the vehicles altitude during entry. In this respect the Surveyor system is different, since the Surveyor has a nominal -90° flight path angle with a $\pm$ 45° variation.

Following main retro ignition the thrust axis is aligned with the computed velocity vector from the Surveyor type RADVS. When the reference contour is reached, Figure (23), throttling will commence to maintain zero altitude and velocity errors with the reference contour as previously discussed. The dynamic pressures at reference contour encounter will be quite low so attitude changes will require small propulsion penalties. At about 500 to 700 fps, the heatshield will be ejected in preparation for the soft touchdown.

CONCLUSIONS

A ballistic entry vehicle with a ballistic parameter of .8 slugs/ft^2 appears to be a suitable configuration for soft landing an MSSR type payload on the Martian surface. For current storable propellant combinations, the payload fraction would be about 36% of the entry weight with a propulsion system fraction of 26% at a thrust-to-weight ratio of 1.5. Thrust-to-weight can be reduced at the expense of increased propellant. Although landed payload fractions can be increased by using parachutes, the 10-to-15% gain may not be worth the additional complexity of the parachute system.

The maximum aerodynamic deceleration loads during entry can be kept below 40 earth gee's. The radiation stagnation heating is considerably less than the convective heating, but the total distributed radiation load is about one half the convective load.

Drag attenuation due to forward firing rocket jets is an open question. It appears, however, that centerline jets reduce drag and peripherally arranged jets increase drag. The effects, though, are a function of the jet total pressure to the free stream total pressure ratio. If, indeed, drag is appreciably reduced during rocket firing, lower altitude ignition and higher thrust-to-weight ratios are required.

For a MSSR type mission, a 4000 pound ascent stage could be delivered to the Martian surface with a 20 foot diameter, 60° blunted cone entry vehicle, and an entry weight on the order of 11,000 pounds.

D. E. Cassidy

1013-DEC-pdm

Attachments
References 1 - 11
Figures 1 - 23

REFERENCES

1. "Atmospheric Data to Alter Voyager Design," Aviation Week and Space Technology, pp. 66-69, dated November 22, 1965.

2. "Venus and Mars Nominal Natural Environments for Advanced Manned Planetary Mission Programs," by D. E. Evans, D. E. Pitts, and G. L. Krus, NASA SP-3016, dated, 1967.

3. "Navigation and Guidance Analysis of a Mars Probe Launched from a Manned Flyby Spacecraft," by T. B. Murtagh, F. B. Lowes, and V. R. Bond, AIAA Paper No. 67-546, AIAA Guidance, Control, and Flight Dynamics Conference, Huntsville, Alabama, August 14 - 16, 1967.

4. "Aerothermodynamics of Planetary Entry," J. M. Spiegel, F. Wolf, and T. Horton, Jet Propulsion Laboratory, Solar Probe Spacecraft Report SPS 37-22, Vol. IV, Section 354, dated August 31, 1963.

5. "Compariative Studies of Conceptual Design and Qualification Procedures for a Mars Probe/Lander," Final Report, Avco Corporation AVSSD-0006-66-RR, Contract NAS 1-5224.

6. "Laminar Heat Transfer Over Blunt-Nosed Bodies at Hyperbolic Flight Speeds," L. Lees, Jet Propulsion, April, 1956.

7. "Unmanned Entry Probe Sizing for a 1975 Manned Mars Flyby Mission - Case 103-2," Bellcomm Memorandum for File, by D. E. Cassidy, dated July 11, 1966.

8. "Some Considerations for Reducing the Size of Unmanned Mars Entry Probe Packages - Case 103-2," by D. E. Cassudy, dated July 28, 1966.

9. "Conceptual Design of a Structural and Propulsion Systems for an MSSR Rendezvous Vehicle - Case 103-2," by D. Macchia, M. H. Skeer, and J. Wong, dated August 5, 1966.

10. "Effects of Simulated Retrorocket on the Aerodynamic Characteristics of a Body of Revolution at Mach Numbers from .25 to 1.9," by V. L. Peterson and R. L. McKenzie, NASA TN D-1300, dated May, 1962.

11. "Effects of Forward-Facing Jets on Aerodynamic Characteristics of Blunt Configurations at Mach 6," by J. Wayne Keyes and J. M. Helner, Engineering Note AIAA, J., Spacecraft and Rockets, dated April, 1967.

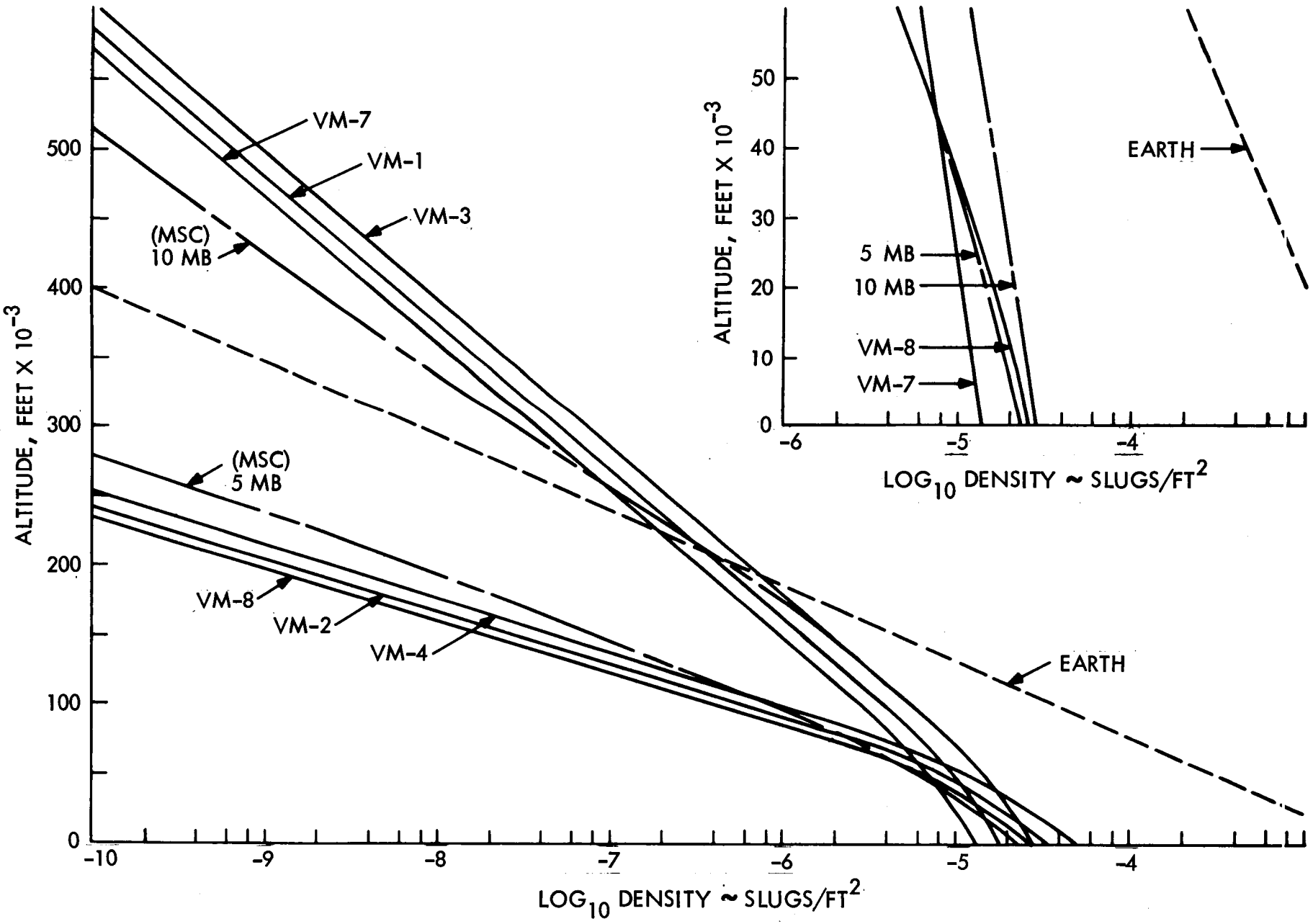

FIGURE 1. MARS MODEL ATMOSPHERES, DENSITY

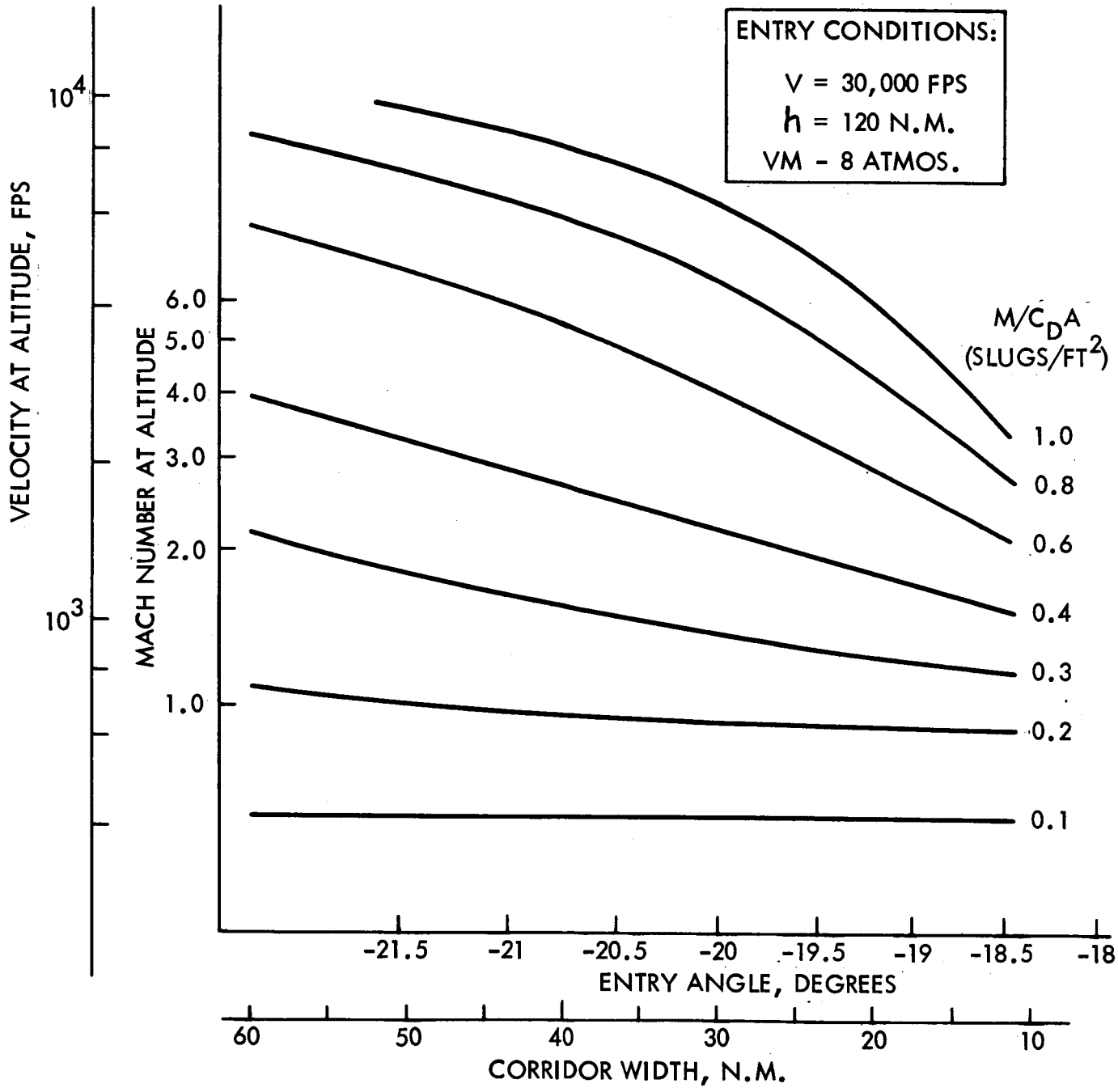

FIGURE 2. VELOCITY AT 20,000 FT. ALTITUDE FOLLOWING BALLISTIC ENTRY

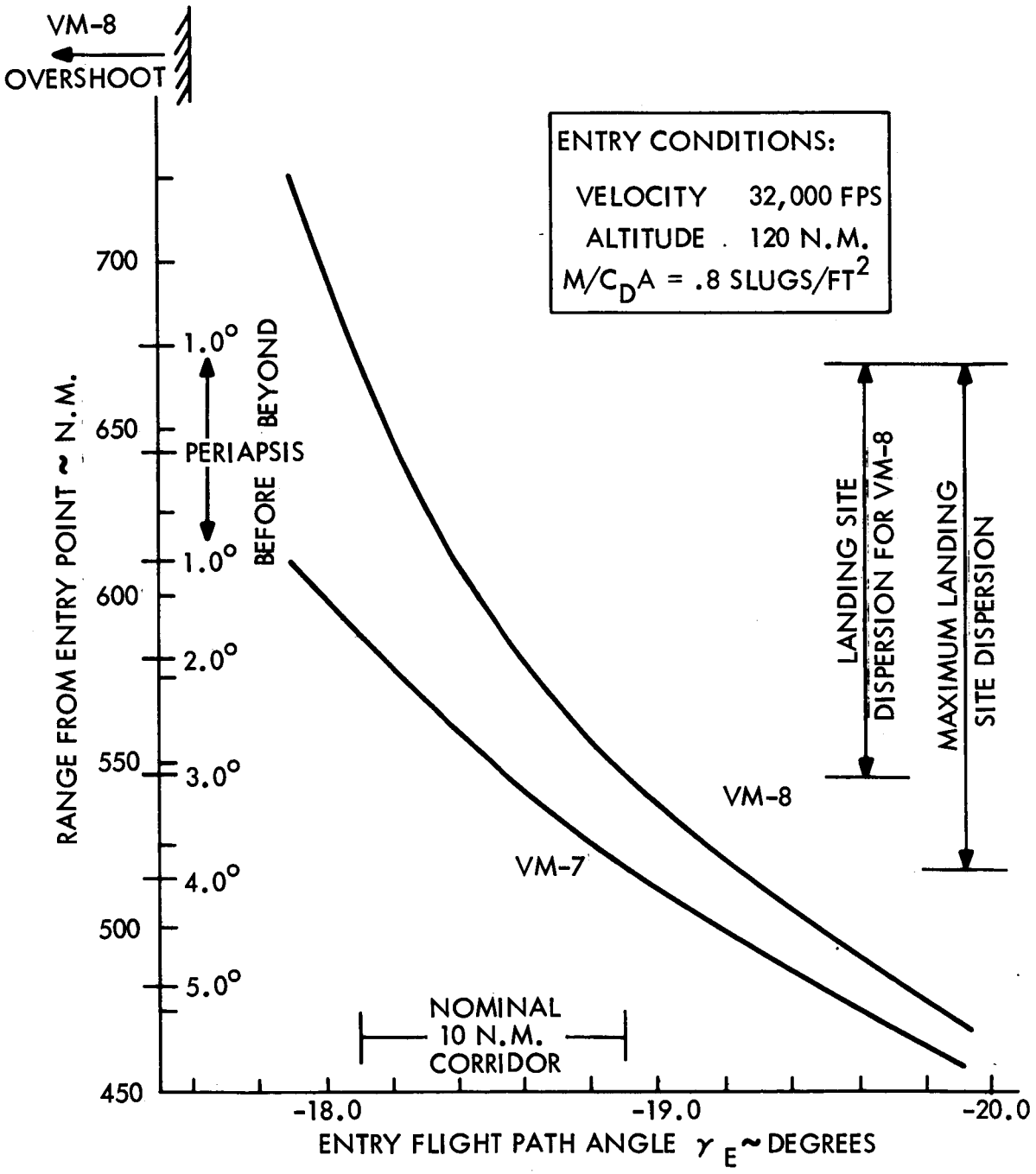

FIGURE 3. RANGE VARIATIONS DUE TO ENTRY CORRIDOR AND ATMOSPHERIC UNCERTAINTIES

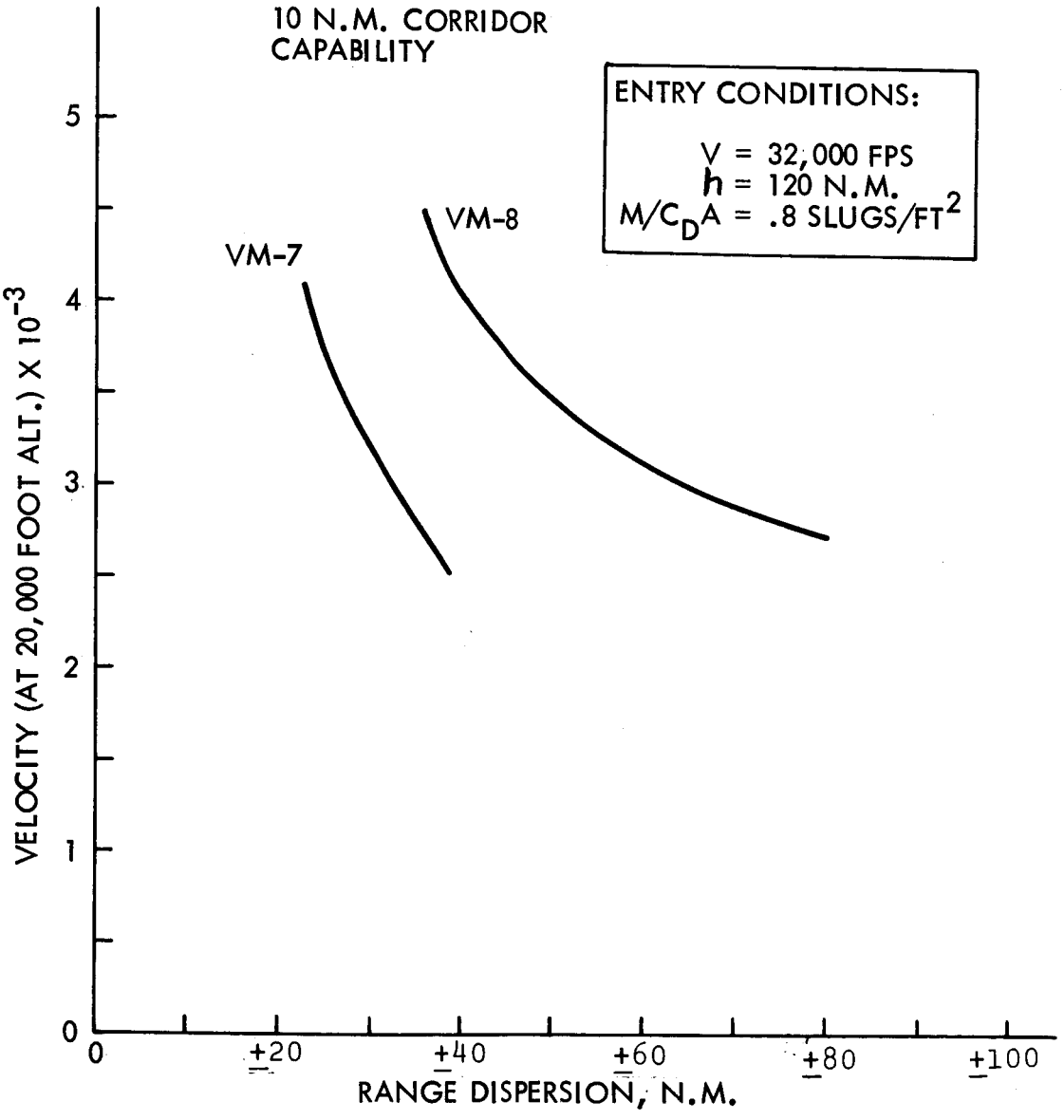

FIGURE 4. VELOCITY AT 20,000 FOOT ALTITUDE VS. RANGE DISPERSION

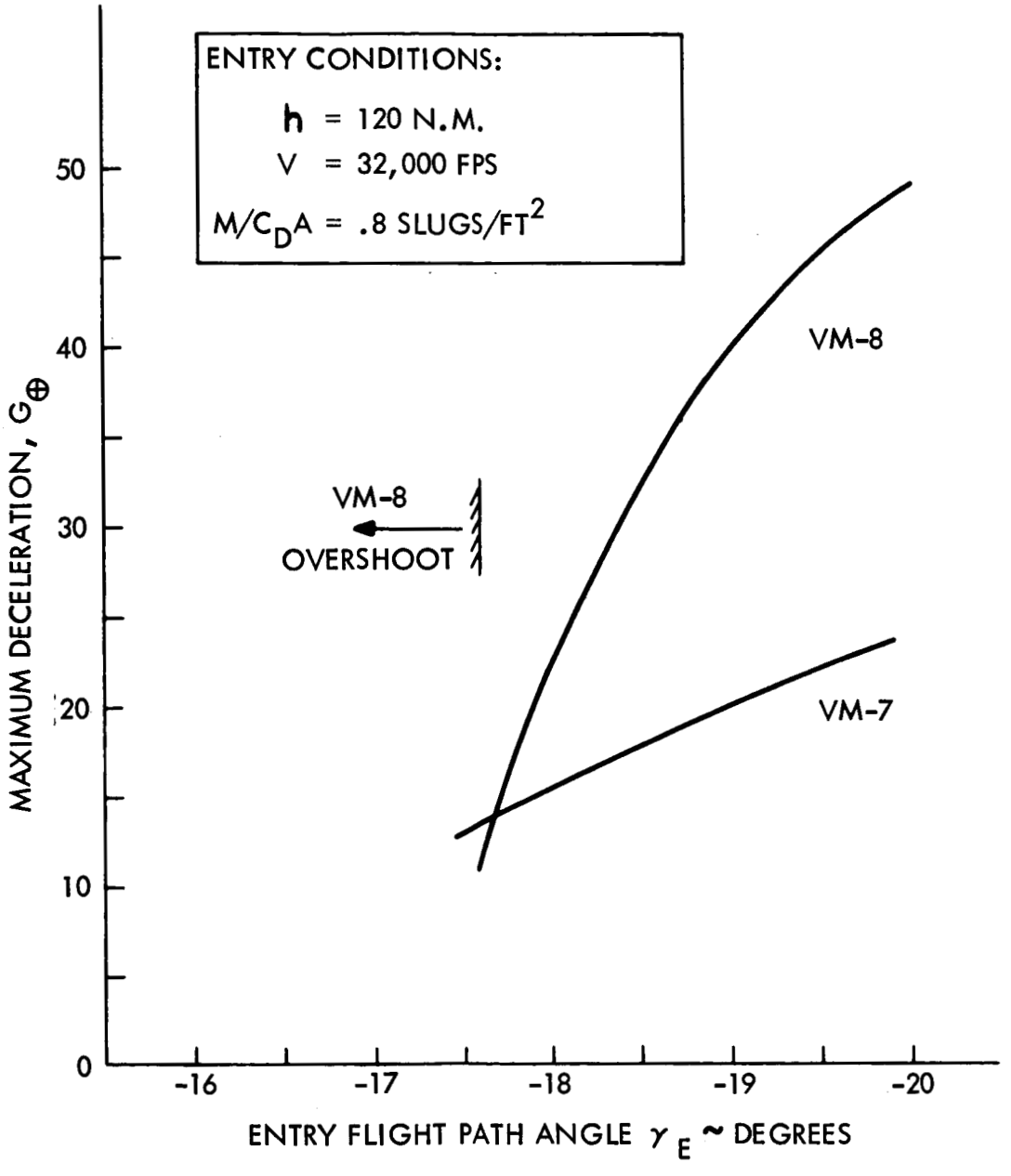

FIGURE 5. MAXIMUM DECELERATION

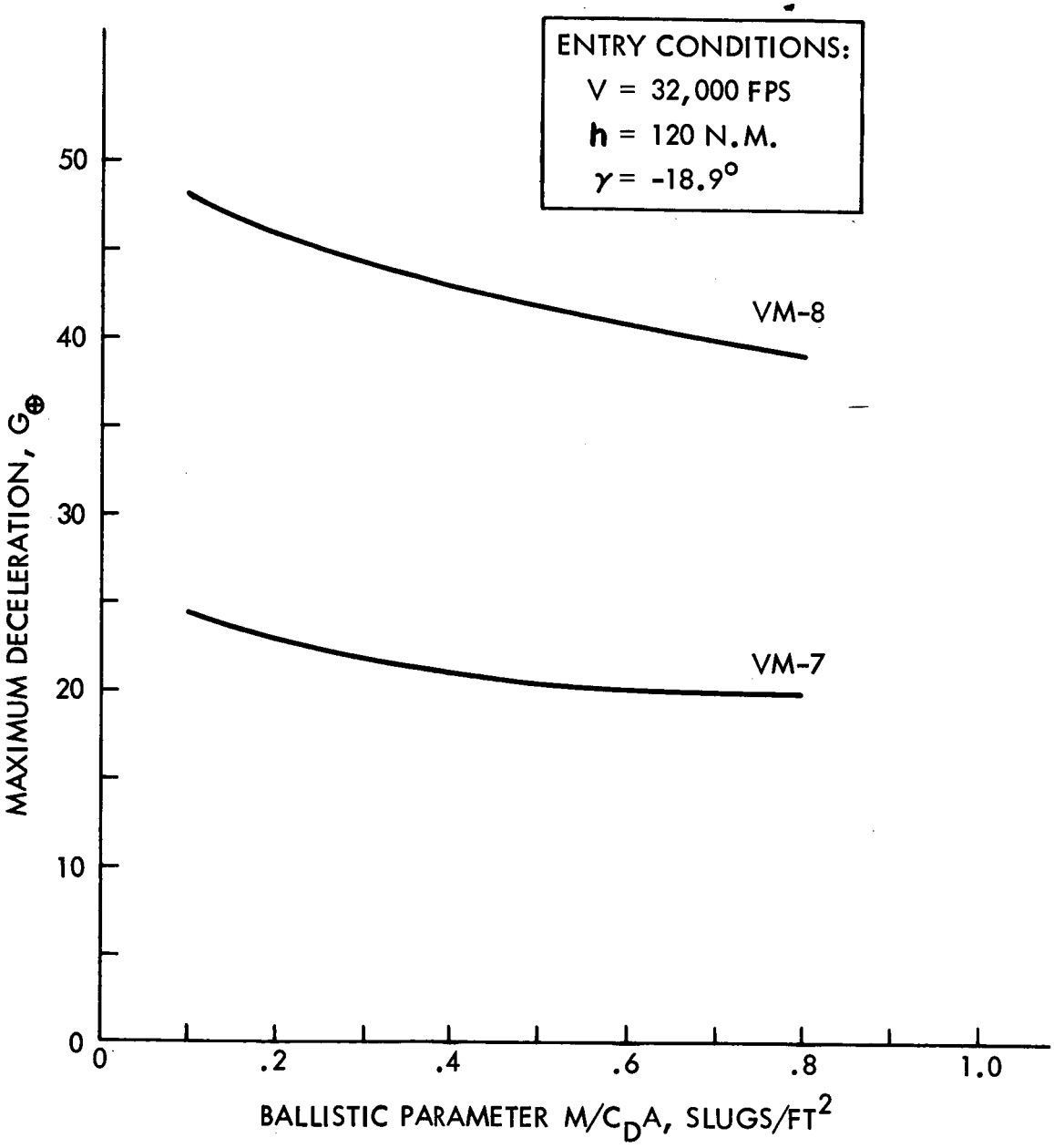

FIGURE 6. MAXIMUM DECELERATION

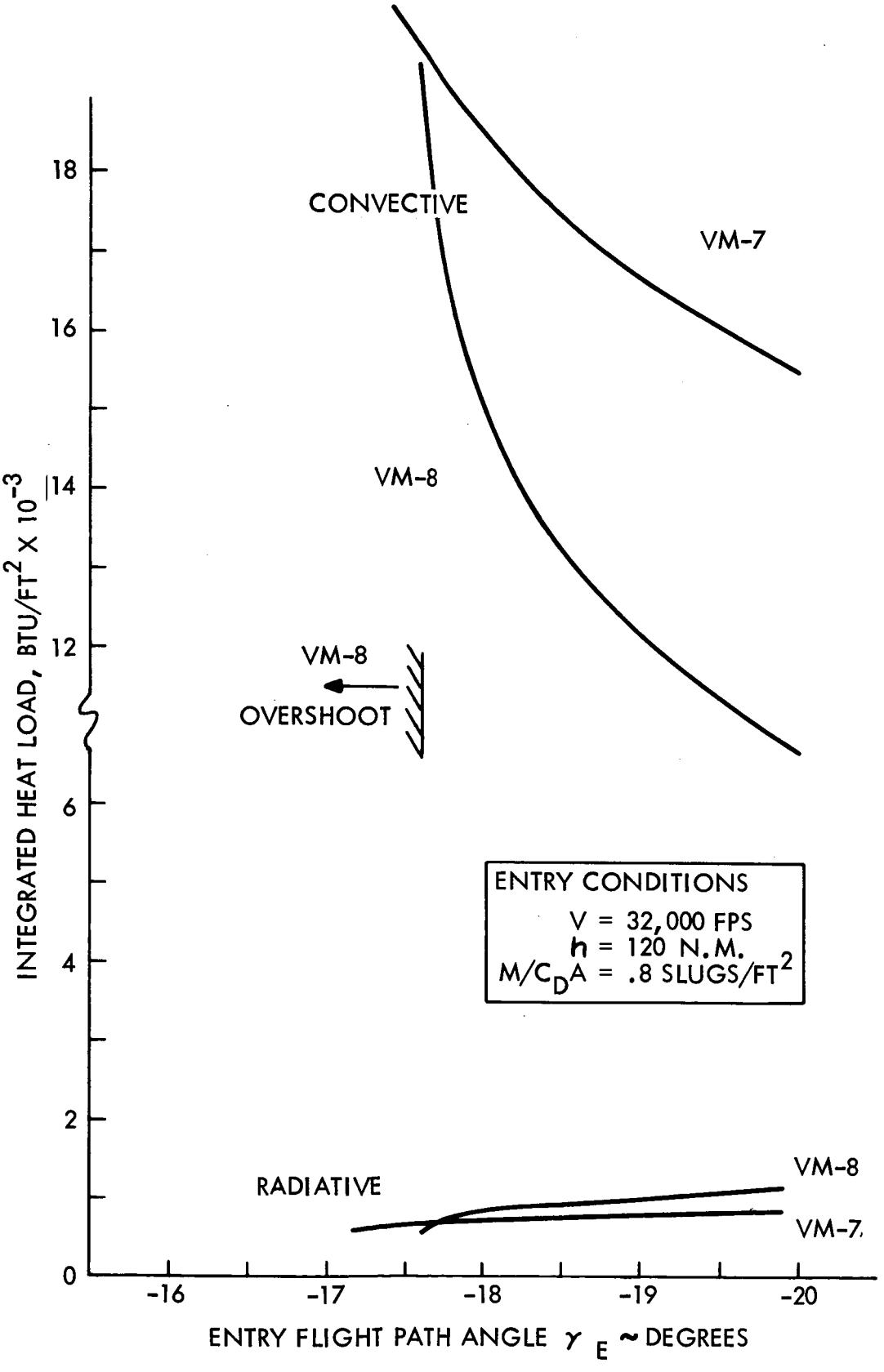

FIGURE 7. HEAT LOAD TO STAGNATION POINT OF 1 FOOT RADIUS

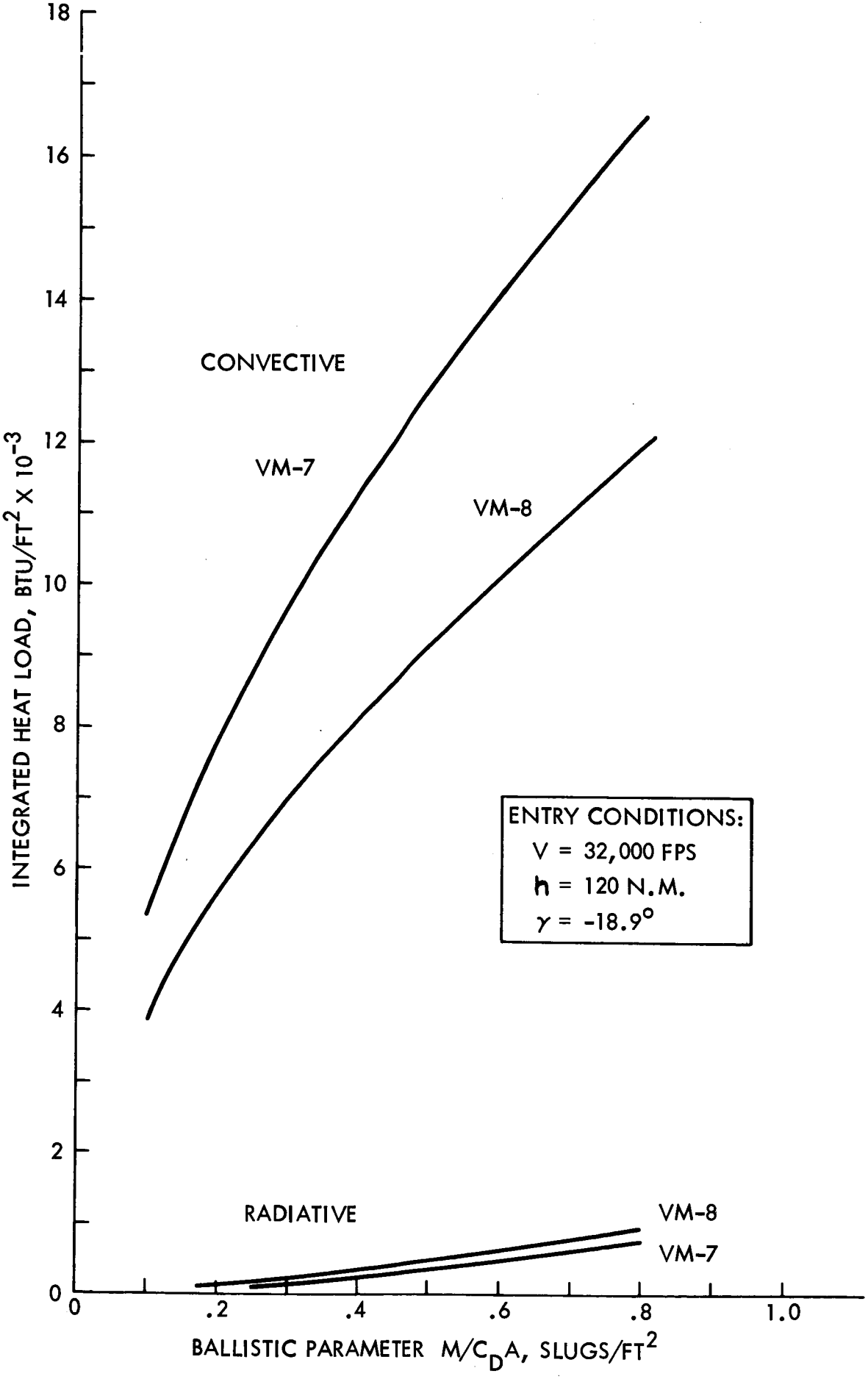

FIGURE 8. INTEGRATED HEAT LOAD TO STAGNATION POINT OF 1 FOOT RADIUS

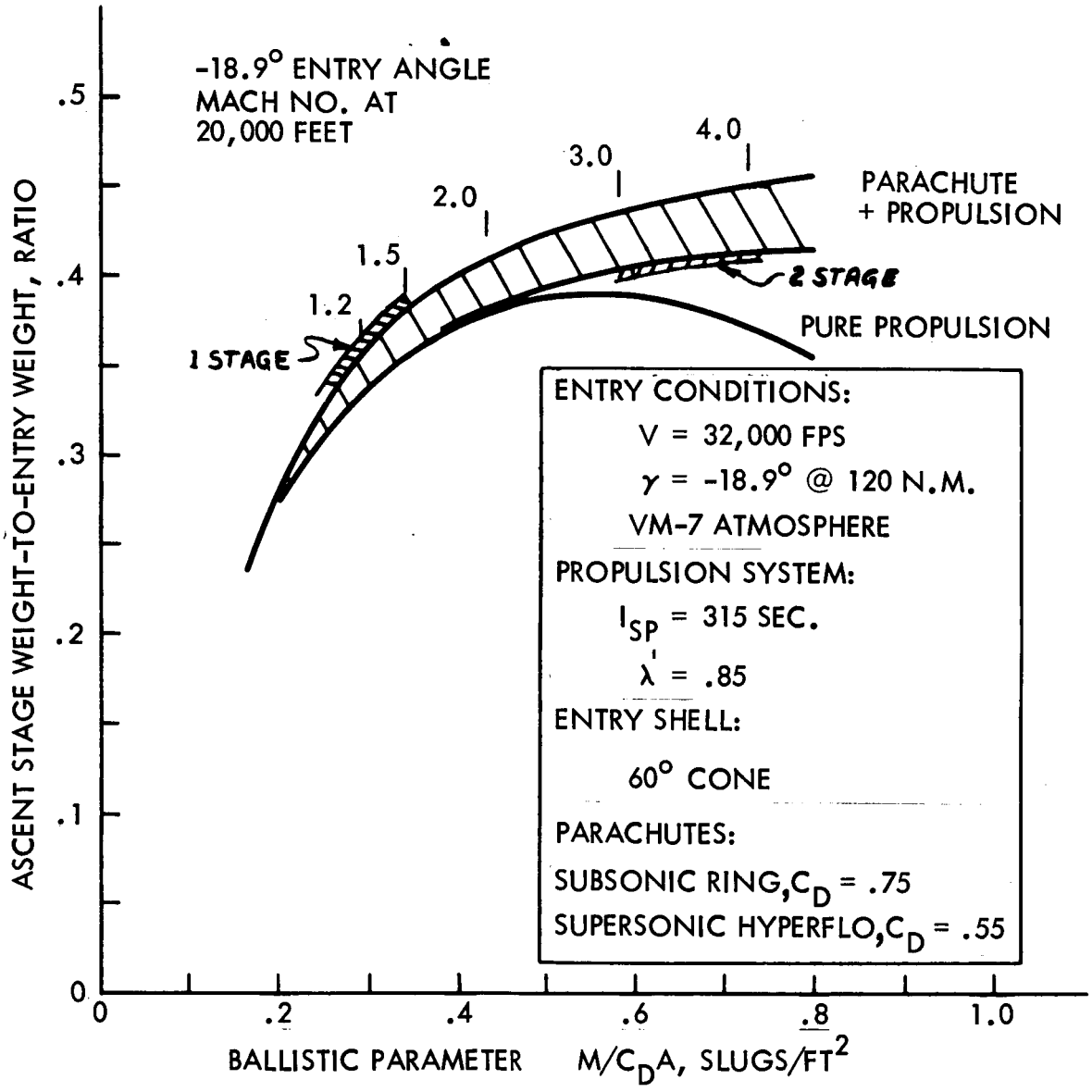

FIGURE 9. ASCENT STAGE FRACTION VS. BALLISTIC PARAMETER

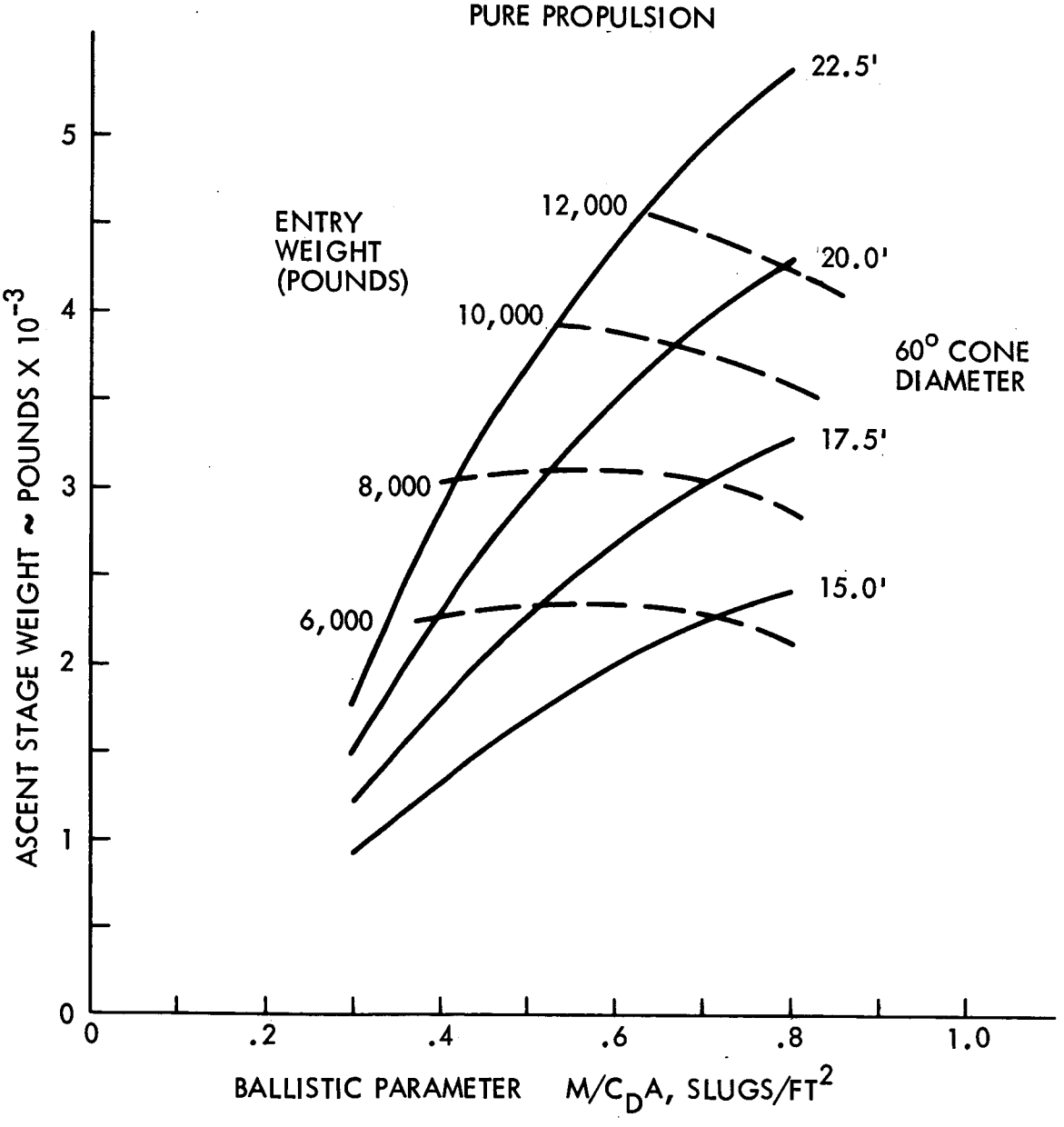

FIGURE 10. ASCENT STAGE WEIGHT VS. BALLISTIC PARAMETER

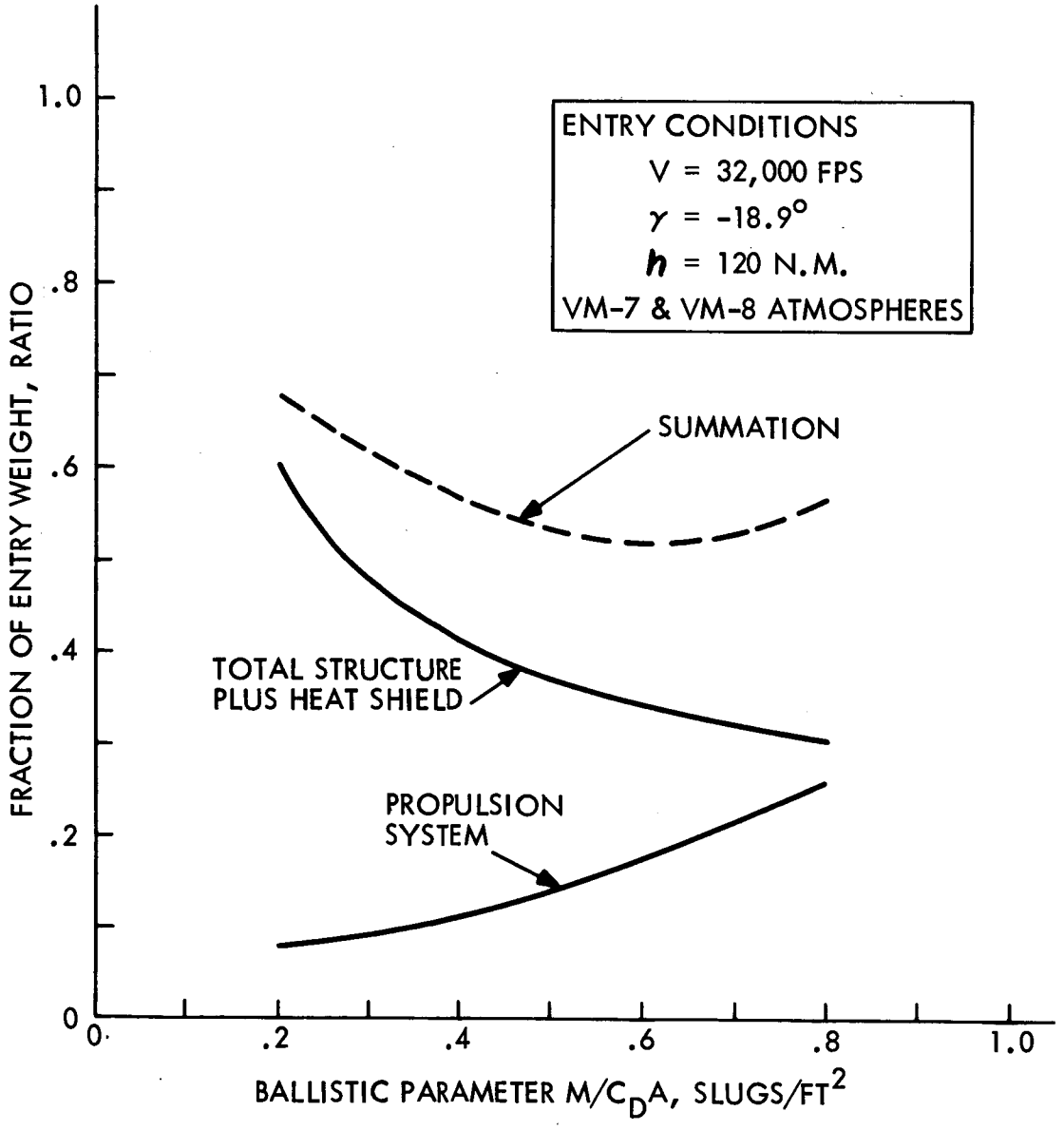

FIGURE 11. TOTAL SHELL STRUCTURE PLUS HEAT SHIELD — AND — PROPULSION SYSTEM FRACTIONS OF ENTRY WEIGHT

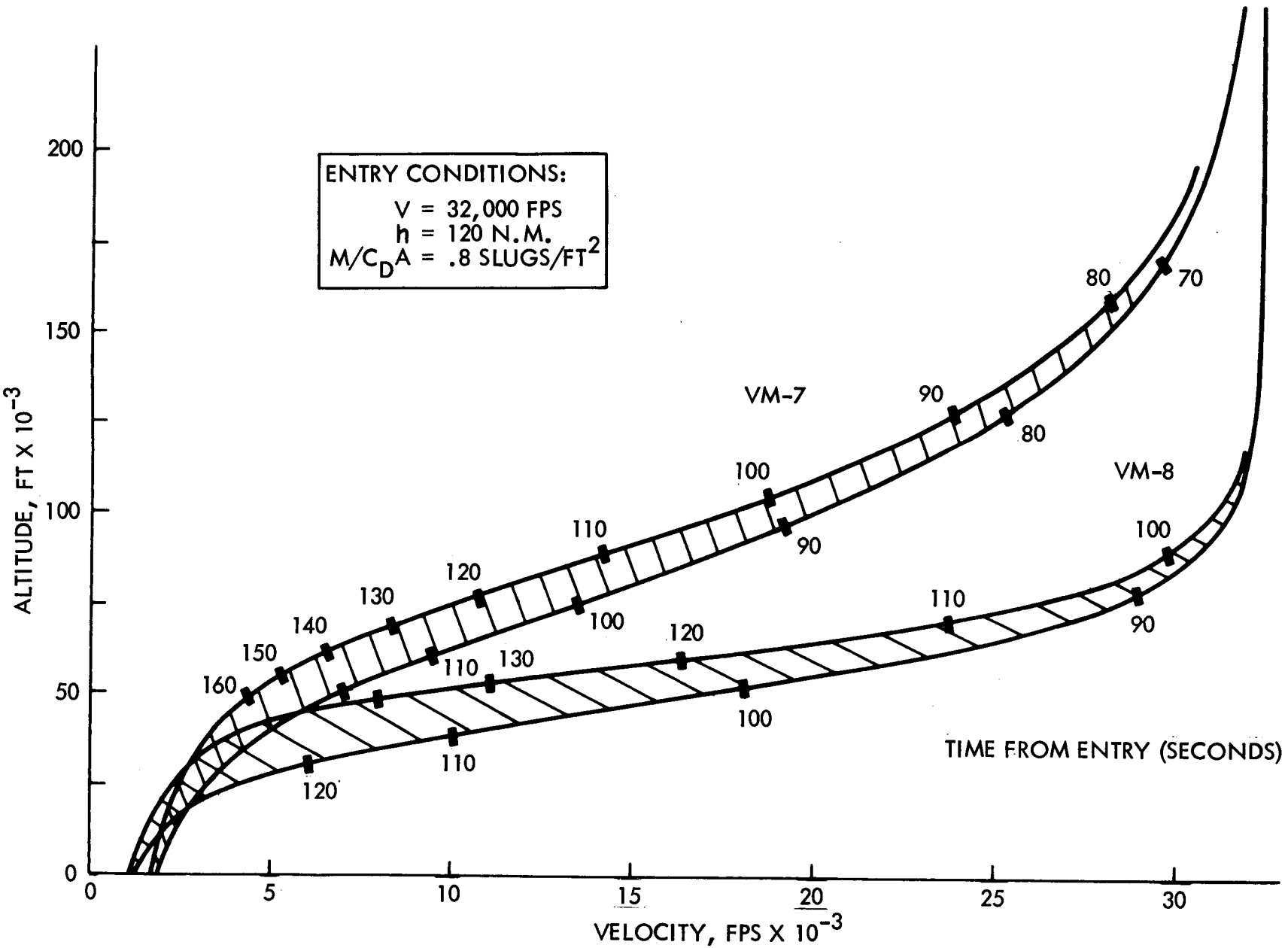

FIGURE 12. ALTITUDE VS. VELOCITY

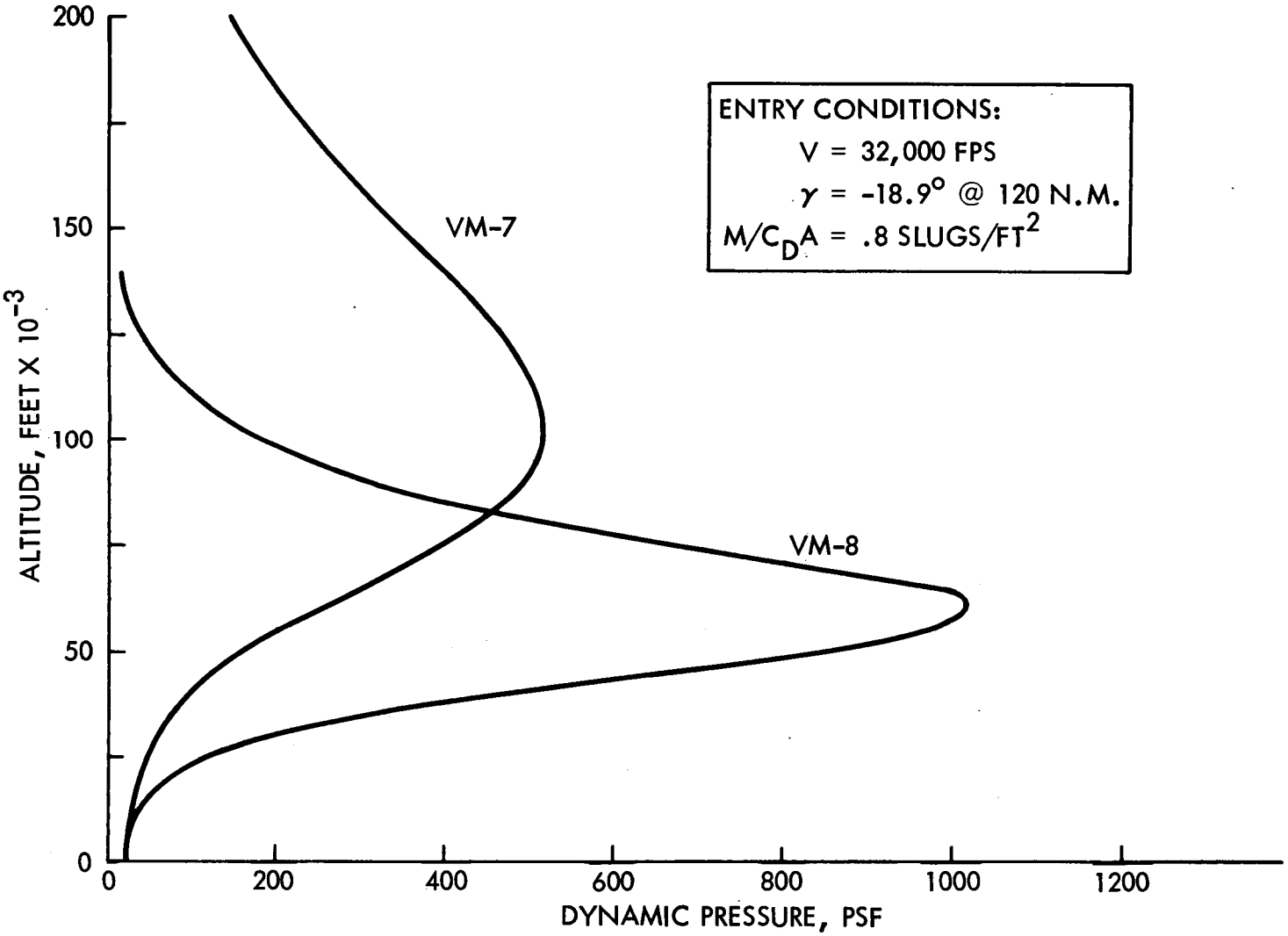

FIGURE 13. ALTITUDE VS. DYNAMIC PRESSURE

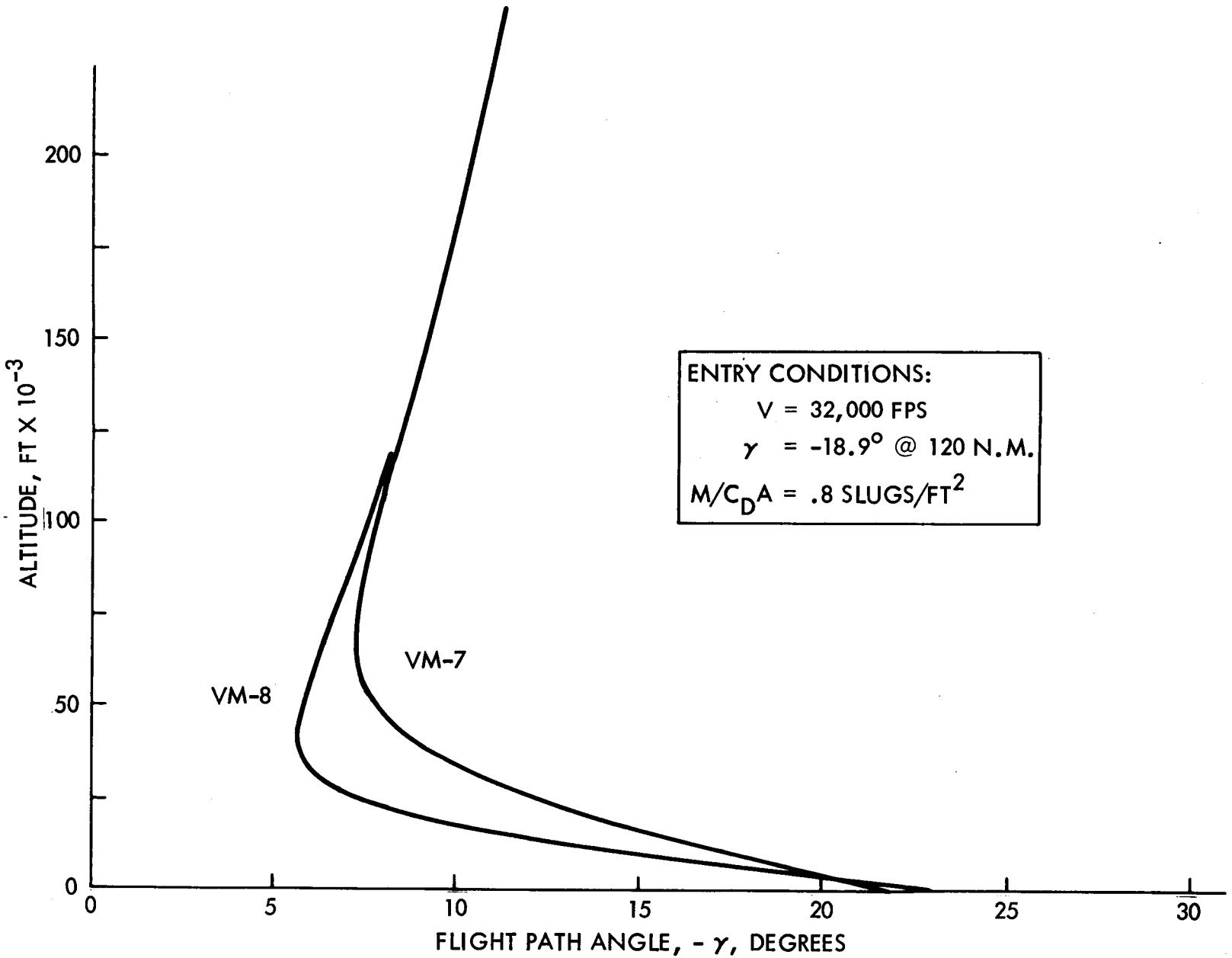

FIGURE 14. ALTITUDE VS. FLIGHT PATH ANGLE

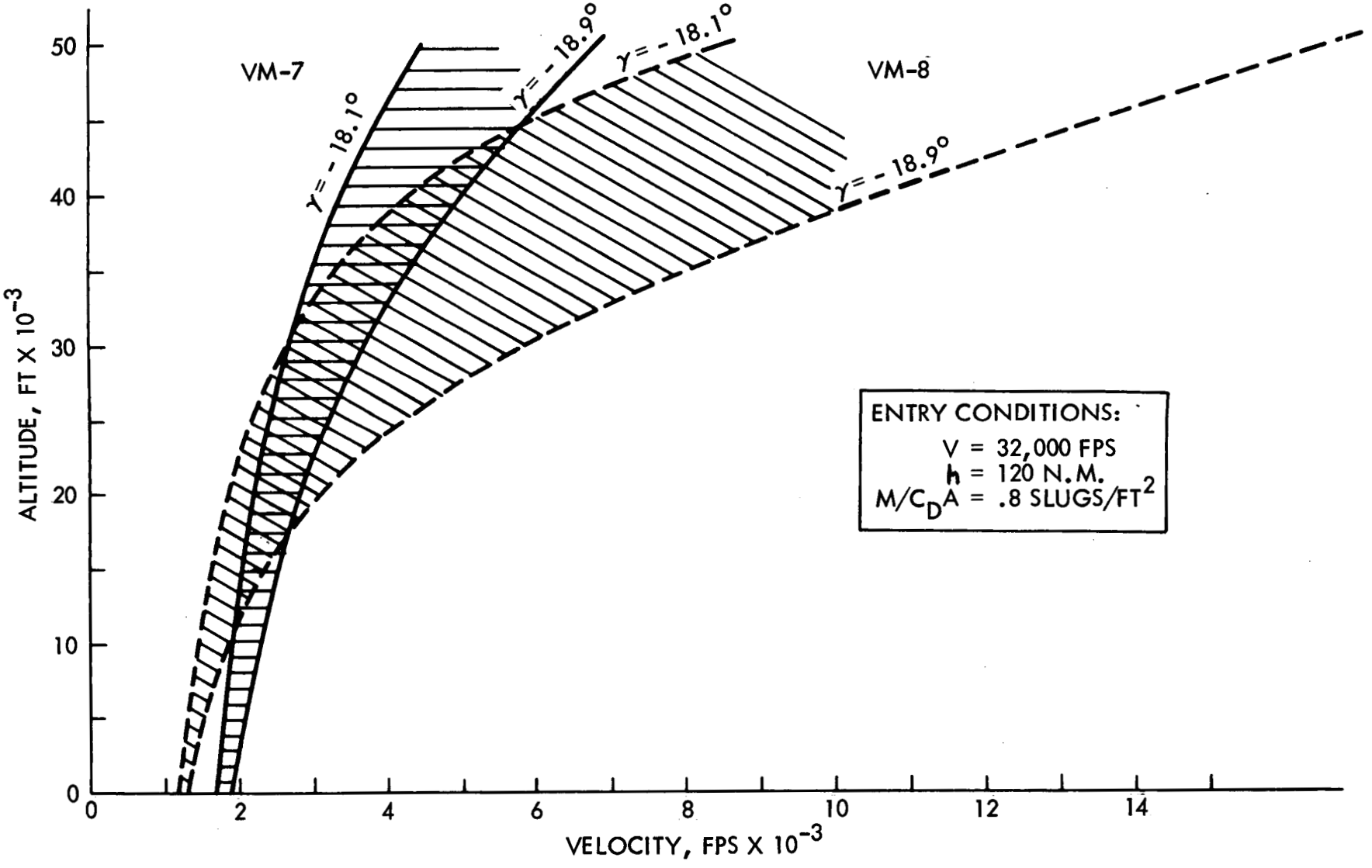

FIGURE 15. ALTITUDE VS. VELOCITY

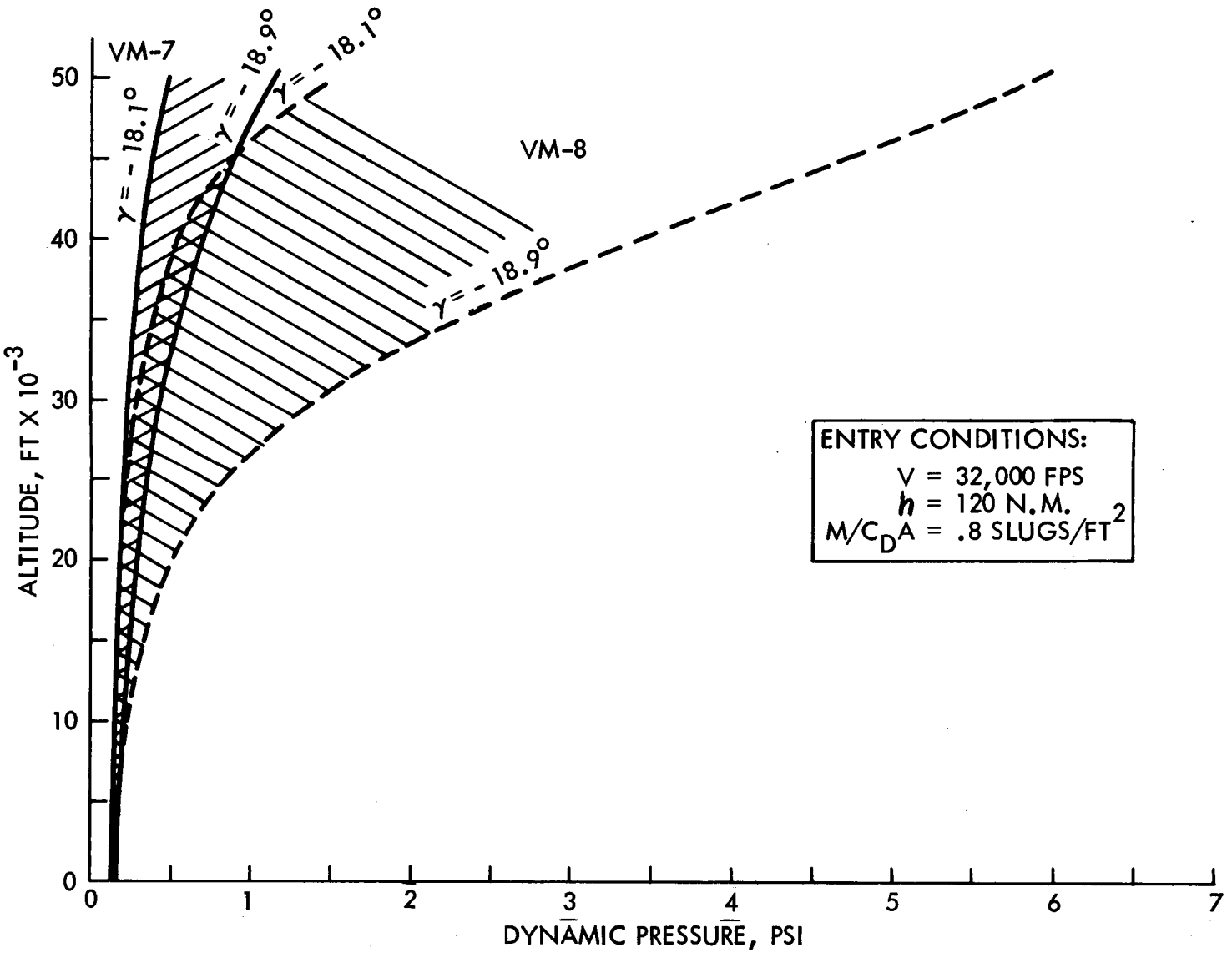

FIGURE 16. ALTITUDE VS. DYNAMIC PRESSURE

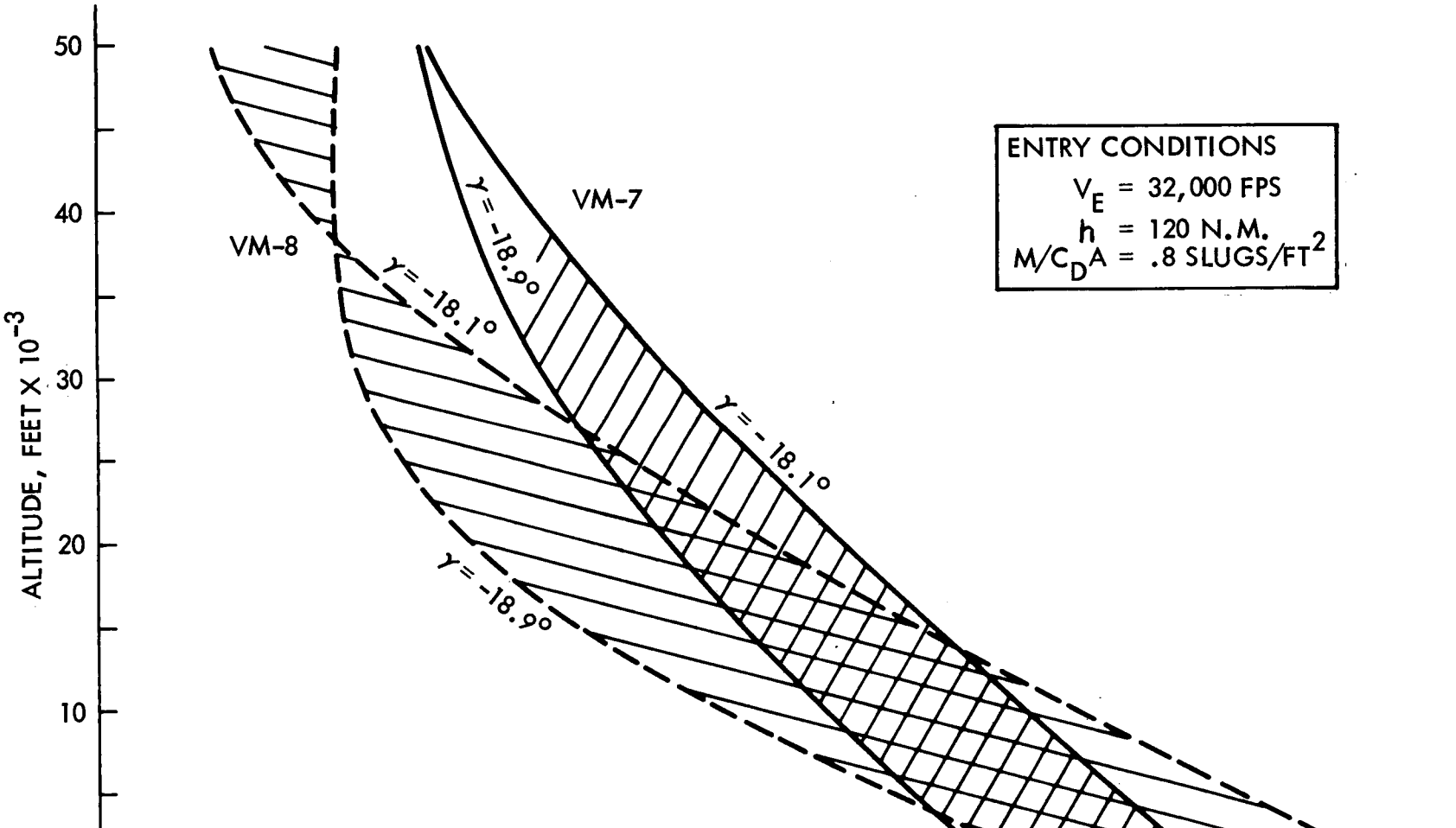

FIGURE 17. ALTITUDE VS. FLIGHT PATH ANGLE

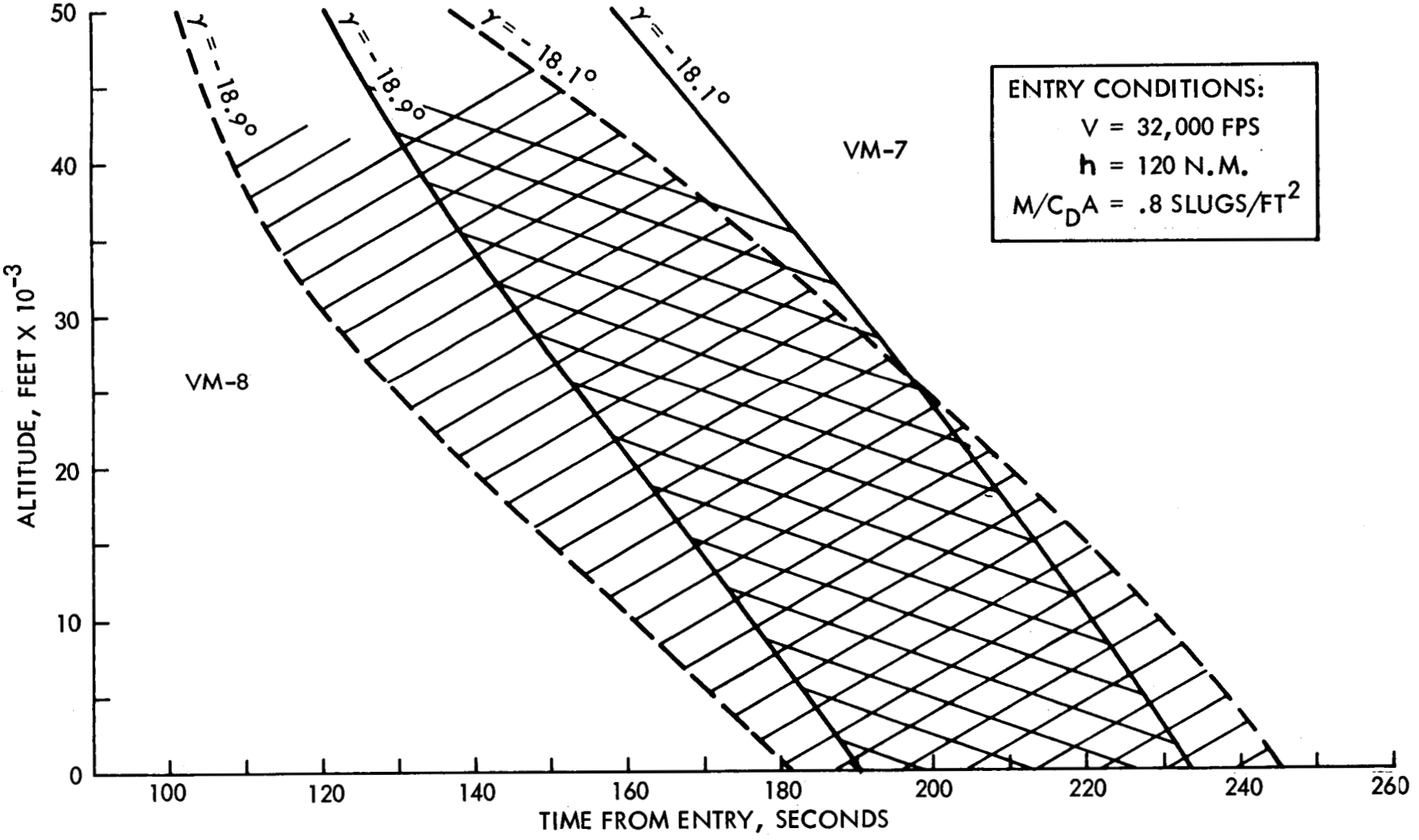

FIGURE 18. ALTITUDE VS TIME FROM ENTRY

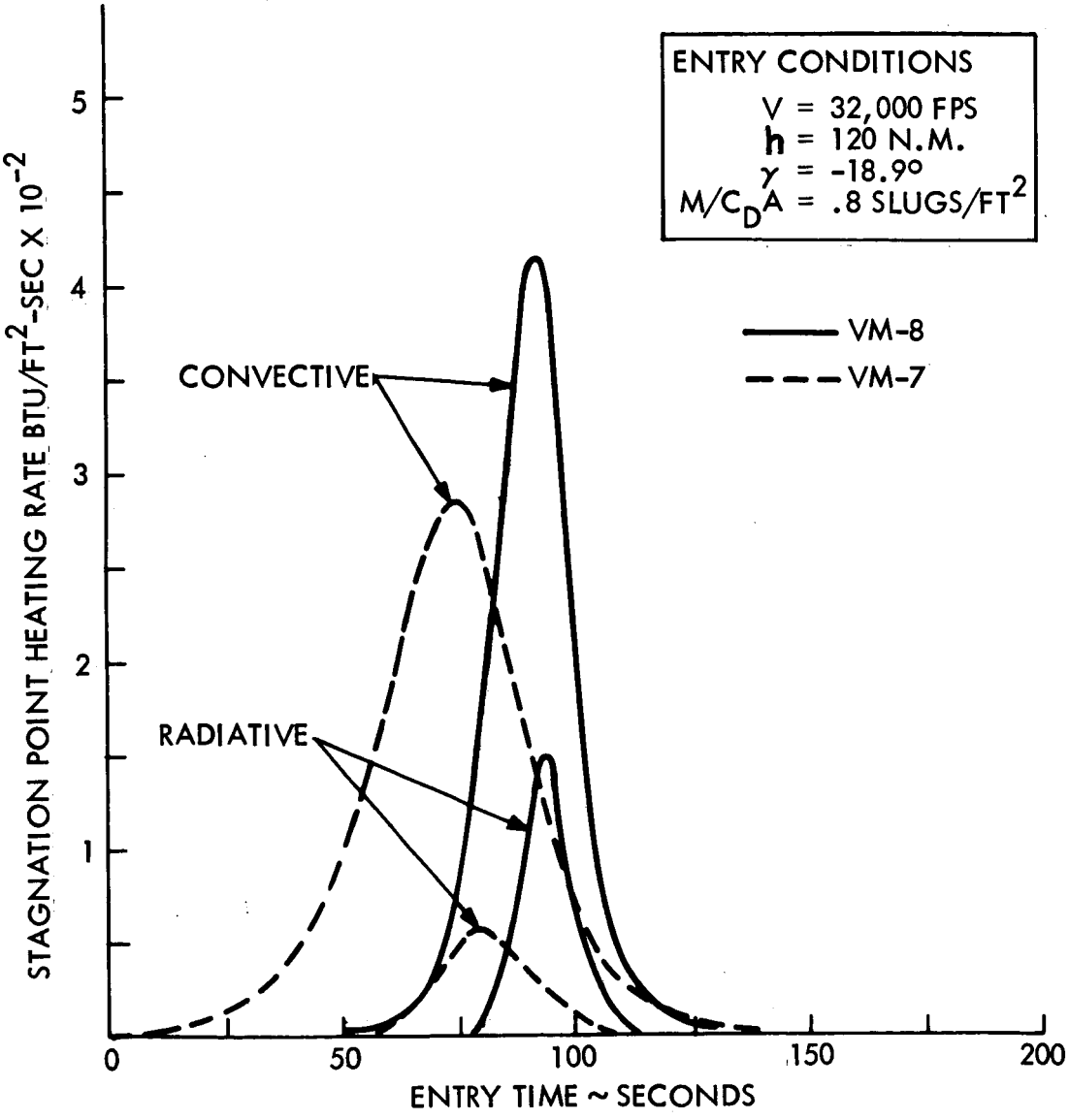

FIGURE 19. STAGNATION POINT HEATING RATE - 2 FOOT NOSE RADIUS

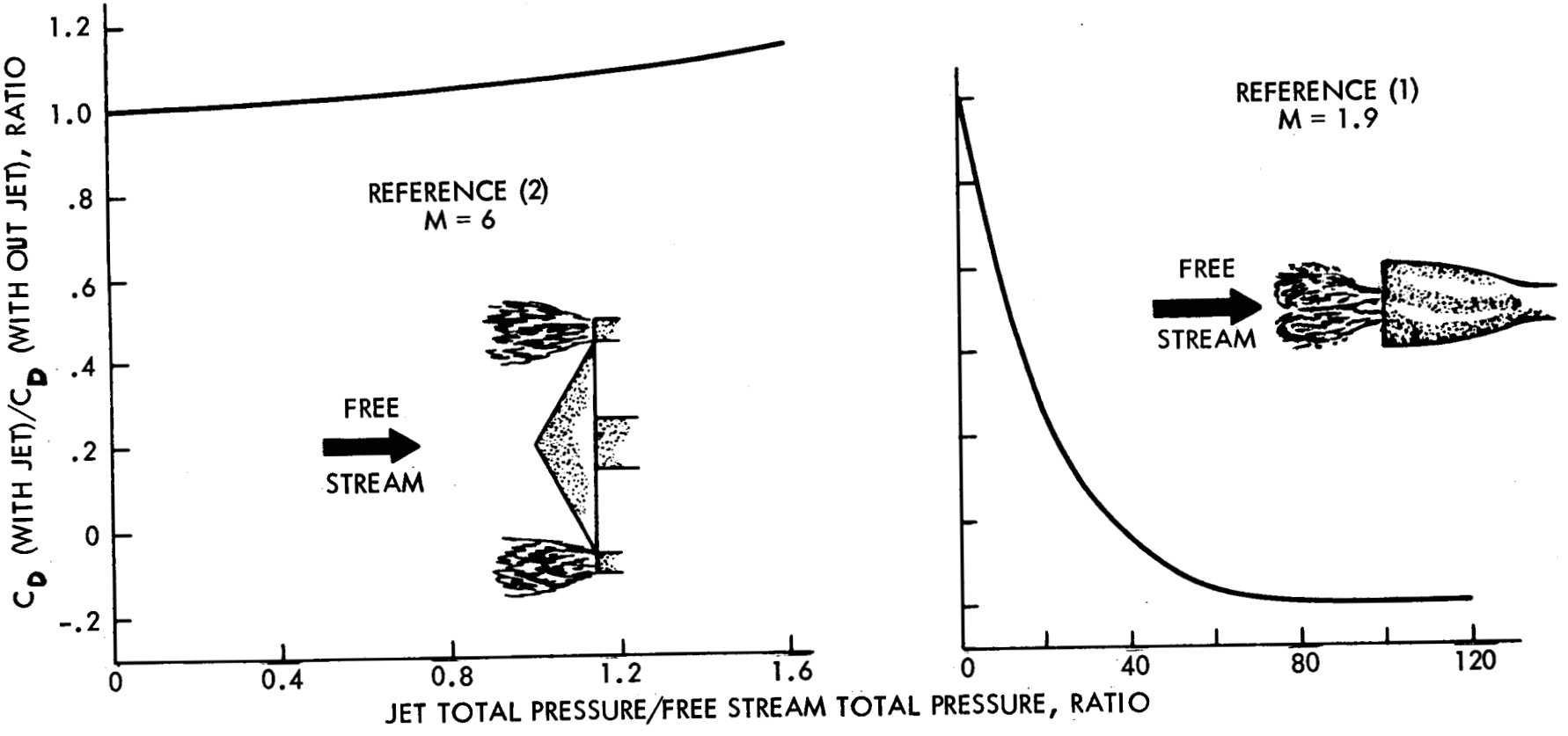

FIGURE 20. EFFECTS OF FORWARD FACING JETS ON DRAG COEFFICIENT (EXCLUDING THRUST FORCE)

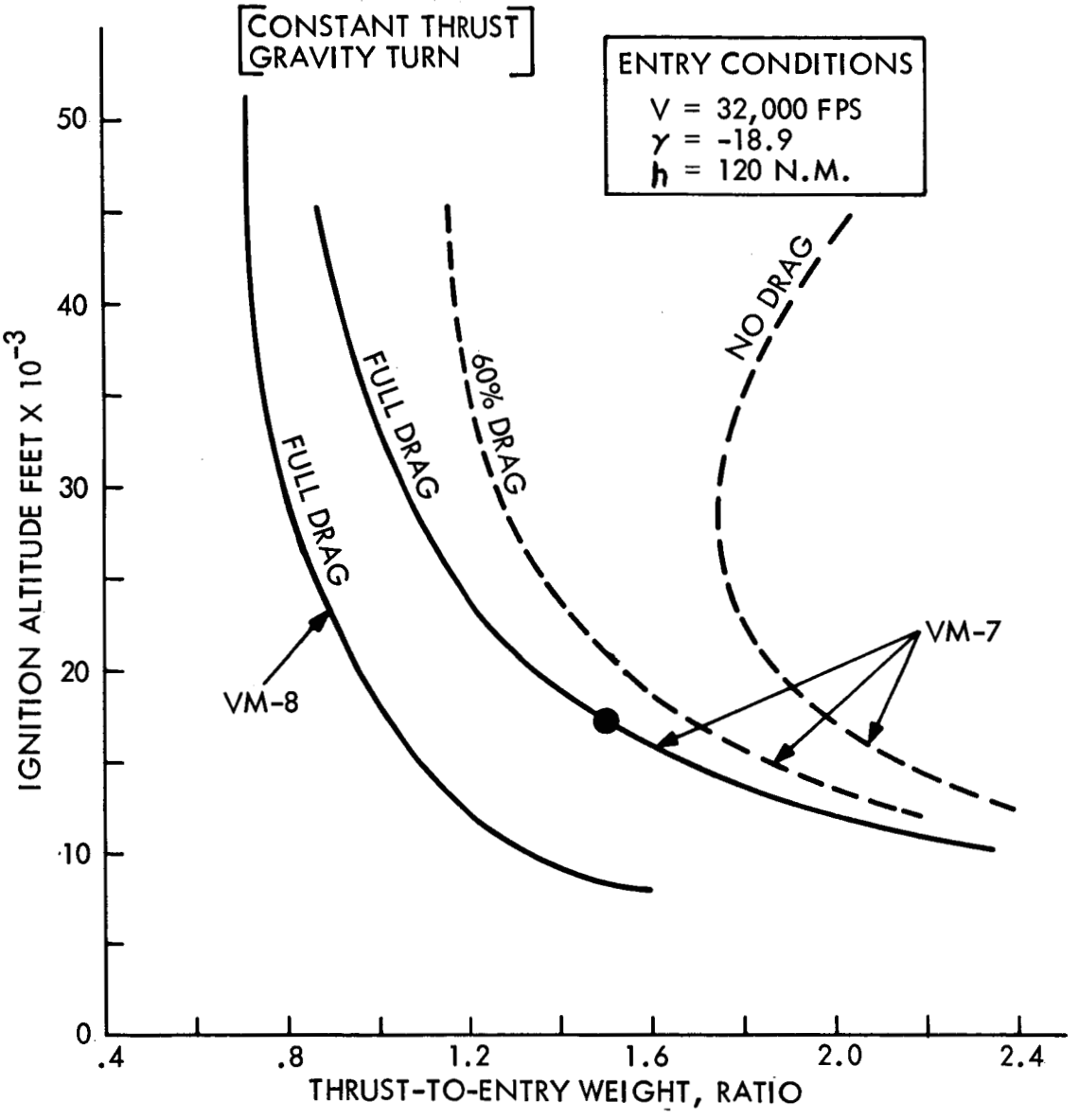

FIGURE 21. IGNITION ALTITUDE VS. THRUST-TO-ENTRY WEIGHT

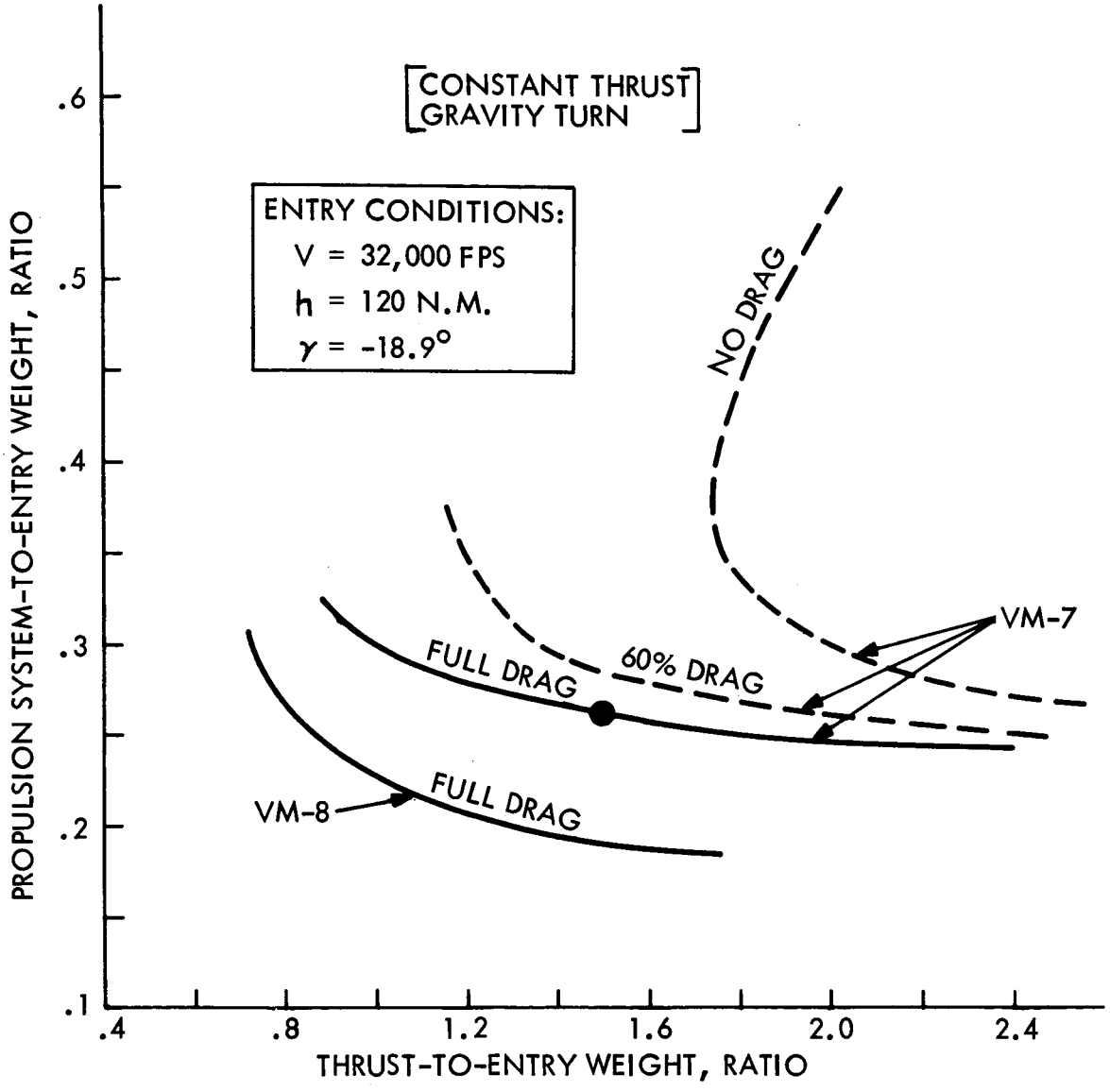

FIGURE 22. PROPULSION SYSTEM FRACTION VS. THRUST-TO-ENTRY WEIGHT

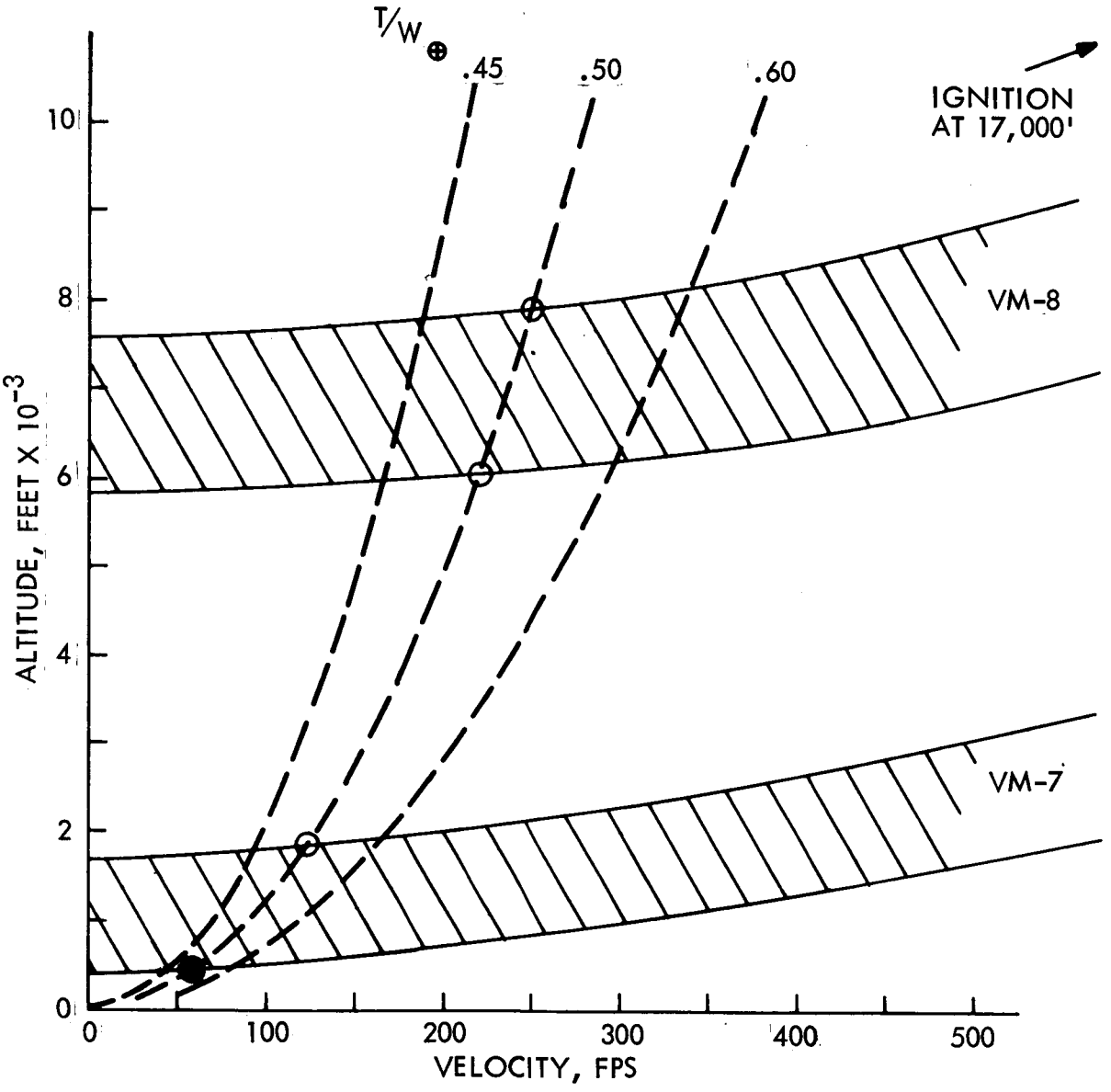

FIGURE 23. TERMINAL DESCENT ALTITUDE VS. VELOCITY